ADAPTIVITY AND A POSTERIORI ERROR CONTROL FOR BIFURCATION PROBLEMS II: INCOMPRESSIBLE FLUID FLOW IN OPEN SYSTEMS WITH Z_2 SYMMETRY

K. ANDREW CLIFFE *, EDWARD J.C. HALL †, PAUL HOUSTON ‡, ERIC T. PHIPPS §, AND ANDREW G. SALINGER ¶

Abstract. In this article we consider the *a posteriori* error estimation and adaptive mesh refinement of discontinuous Galerkin finite element approximations of the bifurcation problem associated with the steady incompressible Navier–Stokes equations. Particular attention is given to the reliable error estimation of the critical Reynolds number at which a steady pitchfork or Hopf bifurcation occurs when the underlying physical system possesses reflectional or Z_2 symmetry. Here, computable *a posteriori* error bounds are derived based on employing the generalization of the standard Dual–Weighted–Residual approach, originally developed for the estimation of target functionals of the solution, to bifurcation problems. Numerical experiments highlighting the practical performance of the proposed *a posteriori* error indicator on adaptively refined computational meshes are presented.

Key words. Incompressible flows, bifurcation problems, *a posteriori* error estimation, adaptivity, discontinuous Galerkin methods, Z_2 symmetry

1. Introduction. Due to the highly nonlinear governing equations and complex geometries involved, understanding fluid flow remains one of the fundamental engineering challenges today. Often it is impossible to obtain analytical solutions to problems and numerical methods must instead be exploited. Broadly speaking, there are two numerical approaches to understanding the Navier-Stokes equations: the first involves direct 'simulation' of the time dependent problem, while the second, less commonly used approach focuses on applying nonlinear analysis to compute paths of steady solutions using numerical continuation methods and to determine their stability based on eigenvalue information. In this article we focus on the latter technique, specifically where we seek to understand how the solution structure changes as one parameter of interest is varied; in the case of the incompressible Navier-Stokes equations this parameter is typically the Reynolds number. We are particularly interested in the location of critical parameters at which a bifurcation first occurs; a review of techniques for bifurcation detection can be found in Cliffe *et al.* [16], for example.

Over the past few decades, tremendous progress has been made in the area of *a posteriori* error estimation and adaptive finite element approximation of partial differential equations; for a review of some of the main developments in the subject we refer to the recent monographs [1, 40, 44], and the articles [22, 10]. Despite a number of significant advances in the field, much of the research to date has focused on source problems. In the context of the finite element approximation of second–order self-adjoint elliptic eigenvalue problems we mention the recent articles [20, 21, 33, 37]; for related work, based on considering the eigenvalue problem as a parameter–dependent

* School of Mathematical Sciences, University of Nottingham, University Park, Nottingham NG7 2RD, UK, email: Andrew.Cliffe@nottingham.ac.uk.
† School of Mathematical Sciences, University of Nottingham, University Park, Nottingham NG7 2RD, UK, email: Edward.Hall@nottingham.ac.uk.
‡ School of Mathematical Sciences, University of Nottingham, University Park, Nottingham NG7 2RD, UK, email: Paul.Houston@nottingham.ac.uk.
§Computer Science Research Institute, Sandia National Laboratories, Albuquerque, New Mexico, email: etphipp@sandia.gov.
¶Computer Science Research Institute, Sandia National Laboratories, Albuquerque, New Mexico, email: agsalin@sandia.gov.

nonlinear equation, see Verfürth [43, 44], for example. For earlier references devoted to the derivation of *a posteriori* error bounds for the finite element approximation of symmetric eigenvalue problems, we refer to [7, 8], for example. Extensions to the finite element approximation of both the eigenvalue problem for the Stokes equations and linear elasticity may be found in the recent articles [36] and [45], respectively. In addition, in [24], the convergence of an adaptive finite element method for the computation of eigenvalues and eigenfunctions of second–order self-adjoint elliptic PDEs is studied. Finally, we mention our recent paper [14], which is concerned with estimating the computational error in critical eigenvalues stemming from the hydrodynamic stability problem. In [14] the dual weighted residual (DWR) error estimation technique is exploited, cf. [9, 29], for example, which is directed at only estimating the error in the given eigenvalue of interest; here the errors stemming from both the approximation of the steady Navier-Stokes equations, as well as those arising from the approximation of the underlying eigenvalue problem itself are included in the resulting error indicators. The natural extension of the DWR *a posteriori* error estimation technique to accurately compute critical parameter values in bifurcation problems has been recently undertaken in [15] for the Bratu problem.

In this article, we consider the generalization of the ideas developed in [15] to bifurcation problems arising in incompressible fluid problems in the case when the underlying problem possesses reflectional, or more precisely, Z_2 symmetry. The detection of bifurcation points in this setting is now well understood, for example, see Golubitsky and Schaeffer [25]. For the purposes of this article, we assume that a symmetric steady state solution to the incompressible Navier-Stokes equations undergoes either a steady pitchfork or (unsteady) Hopf bifurcation at the critical value of the Reynolds number Re. Estimation of the critical Re can be undertaken by discretizing a suitable extended system of partial differential equations; see Brezzi *et al.* [11] and Werner and Spence [47] for steady bifurcations and Jepson [31] and Griewank and Reddien [27] for Hopf bifurcations. For discretization purposes we exploit the interior penalty discontinuous Galerkin (DG) method [5, 19, 18], primarily due to the benefits in mesh adaptivity it affords us. The derivation of a computable error estimator for the critical parameter of interest, namely Re, based on exploiting the DWR *a posteriori* error estimation technique is undertaken and implemented within an adaptive finite element algorithm. The application of this approach to both steady pitchfork and Hopf bifurcations clearly highlight the numerical performance of the error estimation techniques developed in this article. To the best of our knowledge, our article represents the first attempt to derive *a posteriori* error bounds on critical parameter values for the hydrodynamic stability problem in the Z_2 setting; coupling this with the use of DG methods makes this work extremely novel.

This article is structured as follows. In the next section we discuss the general approach adopted for detecting the location at which a bifurcation may occur from the steady state solution of an abstract time dependent problem; we then show how we can utilize any symmetry in the underlying geometry of the problem to reduce the overall computational complexity. Assuming a finite element type discretization of the underlying bifurcation problem, we then proceed in Section 3 to describe how the DWR *a posteriori* error estimation technique can be exploited to approximate the error between the true critical parameter and the computed one. A detailed discussion concerning the reduction of the computational complexity of the discretized bifurcation problem and the associated (discretized) dual problem in the presence of Z_2 symmetry then follows in Section 4. We then turn our attention to the specific

problem of hydrodynamic stability in geometries with Z_2 symmetry; this includes the formulation of the DG discretization of the incompressible Navier-Stokes equations and their appropriate linearization. In Section 7 we investigate the practical performance of the proposed *a posteriori* error estimator on sequences of adaptively generated meshed. In particular, the quality of the (approximate) error representation and (approximate) *a posteriori* bound are studied through two numerical examples. Finally, we summarize the work presented in this article and draw some conclusions in Section 8.

2. Detecting steady and Hopf bifurcation points. Suppose we have a nonlinear, time dependent problem of the form

$$\frac{\partial u}{\partial t} + F(u, \lambda) = 0, \tag{2.1}$$

where F is a map from $V \times \mathbb{R} \to V$, for some Banach space V, with norm $\|\cdot\|$. Here, λ is some distinguished parameter, *e.g.*, the flow rate or Reynolds number, and u is a state variable, *e.g.*, the temperature or velocity field. Our goal is to investigate the linear stability of steady state solutions of (2.1), or more specifically to locate the critical parameter value at which solutions lose stability and bifurcations occur. Before we proceed we make the assumption that F is smooth, that is, F is a C^p mapping with $p \geq 3$. We denote the Fréchet derivative of F with respect to u at a fixed point $(w, \chi) \in V \times \mathbb{R}$ by $F'_u(w, \chi; \cdot)$ and similarly the derivative with respect to λ by $F'_\lambda(w, \chi)$. Here and throughout this article, we use the convention that in semi-linear forms such as $F'_u(\cdot, \cdot; \cdot)$ the form is linear with respect to all arguments to the right of the semicolon. We will assume that $F'_u(u, \lambda; \cdot) : V \to V$ is Fredholm of index 0 for all $(u, \lambda) \in V \times \mathbb{R}$. For convenience, at a given point (u^0, λ^0), we define

$$F^0 := F(u^0, \lambda^0),\ F^0_u(\cdot) := F'(u^0, \lambda^0; \cdot) \text{ and } F^0_\lambda := F'_\lambda(u^0, \lambda^0).$$

Higher-order Fréchet derivatives are expressed in much the same way; for example, the Fréchet derivative of $F'_u(w, \chi, \cdot)$ with respect to u at a fixed point v is denoted by $F''_{uu}(w, \chi; \cdot, v)$ and similarly, at a given point (u^0, ϕ^0, λ^0), we define

$$F^0_{uu}\phi^0(\cdot) := F''_{uu}(u^0, \lambda^0; \cdot, \phi^0) \text{ and } F^0_{u\lambda}\phi^0 := F''_{u\lambda}(u^0, \lambda^0; \phi^0).$$

We investigate the linear stability of steady state solutions u^0 at specific parameter values λ^0, found by solving the steady version of (2.1)

$$F^0 = 0. \tag{2.2}$$

Furthermore, to consider the growth of small perturbations away from u^0, we assume that the solution is of the form $u = u^0 + \phi \mathrm{e}^{-\mu t}$. Thereby, after linearization, from (2.1) we deduce the following eigenvalue problem:

$$F^0_u(\phi) = \mu\phi. \tag{2.3}$$

The nature of the eigenvalues of (2.3) determine the stability of the steady state solution u^0. A change in sign of the real part of any of the eigenvalues from positive to negative indicates a loss of stability; such a set of eigenvalues are referred to as being the *most dangerous* ones. If a single real–valued most dangerous eigenvalue exists, then a steady bifurcation occurs; on the other hand, the presence of a pair of complex conjugate most dangerous eigenvalues indicates a Hopf bifurcation, in which

case a time dependent solution will exist. In [14] we considered the application of the Dual Weighted Residual (DWR) *a posteriori* estimation technique to estimate the error in the computed eigenvalue μ for a series of parameter values λ^0. In contrast, in this article we are now concerned with accurately locating the critical parameter value λ^0 at which a bifurcation first occurs. To this end, for a steady bifurcation we recast equations (2.2)–(2.3) in the following extended system form, where we have dropped the superscript "0" for notational simplicity: find $\mathbf{u}_S := (u, \phi, \lambda)$ such that

$$T_S(\mathbf{u}_S) \equiv \begin{pmatrix} F(u,\lambda) \\ F'_u(u,\lambda;\phi) \\ \langle \phi, g \rangle - 1 \end{pmatrix} = \mathbf{0}, \tag{2.4}$$

where $\langle \cdot, \cdot \rangle$ denotes the duality pairing between the spaces V and V', V' being the dual space of V, and $g \in V'$ is some suitable functional satisfying $\langle \phi, g \rangle \neq 0$. The equation $\langle \phi, g \rangle - 1 = 0$ acts to normalise the nullfunction ϕ, thus ensuring that, if a solution to (2.4) exists at some λ, the solution is unique.

For a Hopf bifurcation we must consider a larger extended system due to the eigenfunction having both a real and complex part; at the critical bifurcation point we make the decomposition $\phi = \phi + \psi i$ and let $\mu = \mu i$, in which case we seek $\mathbf{u}_H := (u, \phi, \psi, \lambda, \mu)$ such that

$$T_H(\mathbf{u}_H) \equiv \begin{pmatrix} F(u,\lambda) \\ F'_u(u,\lambda;\phi) + \mu\psi \\ F'_u(u,\lambda;\psi) - \mu\phi \\ \langle \phi, g \rangle - 1 \\ \langle \psi, g \rangle \end{pmatrix} = \mathbf{0}, \tag{2.5}$$

where $g \in V'$ is a suitable functional satisfying $\langle \phi, g \rangle \neq 0$, in which case a ψ satisfying $\langle \psi, g \rangle = 0$ does exist, see [27].

REMARK 2.1. *We remark that (2.5) will also find a steady bifurcation point, so we must assume that we are looking for a Hopf bifurcation. Werner and Janovsky [46] have considered the alternative extended system: find* $\mathbf{u}_W := (u, \phi, \lambda, \mu)$ *such that*

$$T_W(\mathbf{u}_W) \equiv \begin{pmatrix} F(u,\lambda) \\ F'_u(u,\lambda;F'_u(u,\lambda;\phi)) + \mu\phi \\ \langle g, \phi \rangle \\ \langle g, F'_u(u,\lambda;\phi) \rangle - 1 \end{pmatrix} = \mathbf{0}, \tag{2.6}$$

for suitable g, to locate Hopf bifurcation points. The last equation of (2.6) ensures the solution cannot be a fold point or steady bifurcation. We choose not to exploit this approach, since the term $F'_u(u,\lambda;F'_u(u,\lambda;\phi))$ will lead to a loss of sparsity in the underlying linear system resulting from the linearization of the discretization of (2.6).

Before we embark on the discussion concerning the detection of steady and Hopf bifurcations in the presence of Z_2 symmetry, we state the following lemma, which will prove useful.

LEMMA 2.2 ('ABCD' Lemma). *Let V be a Banach Space and consider the linear operator $M : V \times \mathbb{R} \to V \times \mathbb{R}$ of the form*

$$M := \begin{pmatrix} A & b \\ \langle \cdot, c \rangle & d \end{pmatrix}, \tag{2.7}$$

where $A : V \to V$, $b \in V \backslash \{0\}$, $c \in V' \backslash \{0\}$, $d \in \mathbb{R}$. Then

1. *If A is an isomorphism on V, then M is an isomorphism on $V \times \mathbb{R}$ if and only if $d - \langle A^{-1}b, c\rangle \neq 0$.*
2. *If $\dim\ker(A) = \operatorname{codim}\operatorname{Range}(A) = 1$, then M is an isomorphism if and only if*
   (a) $\langle b, \psi\rangle \neq 0 \quad \forall \psi \in \ker(A')\backslash\{0\}$,
   (b) $\langle \phi, c\rangle \neq 0 \quad \forall \phi \in \ker(A)\backslash\{0\}$.
3. *If $\dim\ker(A) \geq 2$, then M is singular.*

Proof. See Keller [32]. □

2.1. Bifurcation in the presence of Z_2 symmetry. In this section we discuss the computation of both steady pitchfork and Hopf bifurcations in the case when the underlying problem possesses (reflectional) Z_2 symmetry. The importance of symmetry in bifurcation problems is well known and many of the key concepts, including the connection with group representation theory, may be found in the books by Vanderbauwhede [42], Golubitsky and Schaeffer [25], and Golubitsky *et al.* [26]. The essential idea is that under the action of a group and for an appropriately chosen basis, the Jacobian of a nonlinear problem 'block-diagonalizes', which in turn leads to significant computational savings. With this in mind, we recall that $Z_2 = \{I, s\}$ is the simplest Lie-group, where I denotes the group identity operator and s is a reflection, satisfying $s^2 = I$.

In this section we again consider the steady variant of the nonlinear problem (2.1): find u such that

$$F(u, \lambda) = 0,$$

where additionally we assume that F is Z_2 equivariant; cf. below.

DEFINITION 2.3 (Equivariance). *Let ρ_γ be a representation of the action $\gamma \in Z_2$ onto the space V, then the nonlinear operator $F(\cdot,\cdot) : V \times \mathbb{R} \to V$ is Z_2 equivariant if, for all $\gamma \in Z_2$ and $u \in V$,*

$$\rho_\gamma F(u, \lambda) = F(\rho_\gamma u, \lambda). \tag{2.8}$$

We define the symmetric subspace V^s of V by

$$V^s := \{v \in V : \rho_s v = v\},$$

where ρ_s is the representation of the reflection $s \in Z_2$. Analogously, we introduce the antisymmetric subspace V^a of V by

$$V^a := \{v \in V : \rho_s v = -v\}.$$

With this notation, we observe that V may be written as a direct sum of the symmetric and antisymmetric subspaces V^s and V^a, respectively; i.e., $V = V^s \oplus V^a$.

The equivariance condition (2.8) implies that, if u is a solution of $F(u, \lambda) = 0$, then so is $\rho_\gamma u$ for all $\gamma \in Z_2$. Moreover, taking the Fréchet derivative of (2.8) with respect to u gives

$$\rho_\gamma F'_u(u, \lambda; \phi) = F'_u(\rho_\gamma u, \lambda; \rho_\gamma \phi) \quad \forall \phi \in V.$$

In particular, if $u \in V^s$, then $\rho_\gamma u = u$ for all $\gamma \in Z_2$; consequently,

$$\rho_\gamma F'_u(u, \lambda; \phi) = F'_u(u, \lambda; \rho_\gamma \phi) \quad \forall \phi \in V.$$

Thereby, in the case when $u \in V^s$, the linearized operator $F'_u(u,\lambda;\cdot)$ is also Z_2 equivariant.

The key observation essential for reducing the complexity of the underlying bifurcation problem is the following: given a Z_2 equivariant linear operator $A : V \to V$, we note that V^m, $m = s, a$, are invariant subspaces of A, i.e.,

$$A : V^m \to V^m,$$

$m = s, a$, respectively; cf. Aston [6]. Thereby, for $u \in V^s$, the Jacobian operator $F'_u(u,\lambda;\cdot)$ has a diagonal block structure; more precisely, the following result holds.

LEMMA 2.4. *Suppose $u \in V^s$, then μ is an eigenvalue of*

$$F'_u(u,\lambda;\phi) = \mu\phi, \quad \phi \in V,$$

if and only if μ is also an eigenvalue of

$$F'_u(u,\lambda;\phi) = \mu\phi, \quad \phi \in V^m,$$

where $m = s$ or $m = a$.

Hence, we can locate critical parameter values at which symmetric steady state solutions $u \in V^s$ lose stability, by solving the following problems for $m = s, a$. In the case of a steady bifurcation, find $\mathbf{u}_S = (u, \phi, \lambda) \in V^s \times V^m \times \mathbb{R}$ such that

$$T_S(\mathbf{u}_S) \equiv \begin{pmatrix} F(u,\lambda) \\ F'_u(u,\lambda;\phi) \\ \langle \phi, g\rangle - 1 \end{pmatrix} = \mathbf{0}, \tag{2.9}$$

where $g \in (V^m)'$ is some suitable functional satisfying $\langle \phi, g\rangle \neq 0$. The case of a symmetry breaking bifurcation arises when $m = a$. In addition, we assume that we have a pitchfork bifurcation, in which case the following condition also holds

$$\langle F''_{u\lambda}(u,\lambda;\phi) + F''_{uu}(u,\lambda;w,\phi), \varrho\rangle \neq 0, \tag{2.10}$$

where $\varrho \in \ker((F'_u(u,\lambda,\cdot))')$ and $w \in V^s$ solves $F'_u(u,\lambda;w) + F'_\lambda(u,\lambda) = 0$.

In the case of a Hopf bifurcation, we seek $\mathbf{u}_H = (u, \phi, \psi, \lambda, \mu) \in V^s \times V^m \times V^m \times \mathbb{R} \times \mathbb{R}$ such that

$$T_H(\mathbf{u}_H) \equiv \begin{pmatrix} F(u,\lambda) \\ F'_u(u,\lambda;\phi) + \mu\psi \\ F'_u(u,\lambda;\psi) - \mu\phi \\ \langle \phi, g\rangle - 1 \\ \langle \psi, g\rangle \end{pmatrix} = \mathbf{0}, \tag{2.11}$$

for suitable $g \in (V^m)'$, where $m = s, a$. For a Hopf bifurcation to occur, we assume that the following two conditions are also satisfied:

1. $F'_u(u,\lambda;\cdot)$ has two algebraically simple, purely imaginary eigenvalues $\pm i\omega_0$, $\omega_0 \neq 0$, and no eigenvalues of the form $\pm in\omega_0$, $n = 2, 3, \ldots$.
2. The eigenvalues $\pm i\omega_0$ cross the imaginary axis with non-zero speed as λ varies.

When $m = s$, the Hopf bifurcation gives rise to periodic solutions that are symmetric with respect to the reflection. When $m = a$ the periodic solutions have a spatio-temporal symmetry in which a shift by half a period corresponds to a reflection.

In summary, the key observation is that the original problem can be divided up into a series of smaller problems with computationally reduced complexity. We will assume from now on the case of a symmetry breaking bifurcation and hence solve either (2.9) or (2.11) with $m = a$, cf. Section 7.

3. *A posteriori* error estimation. In this section we develop a general theoretical framework for the derivation of computable *a posteriori* bounds for the error in the computed bifurcation point when the extended systems (2.9) and (2.11) are numerically approximated by a general Galerkin finite element method. To this end, we exploit the duality-based *a posteriori* error estimation technique developed by C. Johnson and R. Rannacher and their collaborators. For a detailed discussion, we refer to the series of articles [10, 30, 22, 34].

We begin by first introducing a suitable finite element approximation of the bifurcation problems (2.9) and (2.11). To this end, we consider a sequence of symmetric finite element spaces $V^s_{h,p}$ and antisymmetric finite elements spaces $V^a_{h,p}$ consisting of piecewise polynomial functions of degree p on a partition $\mathcal{T}_h$ of granularity h.

In the case of a steady bifurcation, we find the triple $\mathbf{u}_{S,h} = (u_h, \phi_h, \lambda_h) \in \mathbf{V}_{S,h,p} := V^s_{h,p} \times V^a_{h,p} \times \mathbb{R}$ such that

$$\begin{aligned}\mathcal{N}_S(\mathbf{u}_{S,h}; \mathbf{v}_h) := \hat{\mathcal{N}}(u_h, \lambda_h; v_h) + \hat{\mathcal{N}}'_u(u_h, \lambda_h; \phi_h, \varphi_h) \\ + \chi_h((g, \phi_h) - 1) = 0 \quad \forall \mathbf{v}_h \in \mathbf{V}_{S,h,p},\end{aligned} \tag{3.1}$$

where $\mathbf{v}_h = (v_h, \varphi_h, \chi_h)$, $(\cdot, \cdot)$ denotes the standard L^2–inner product, $\hat{\mathcal{N}}(\cdot, \cdot; \cdot)$ is the semi-linear form associated with the discretization of the underlying steady state partial differential equation (2.2) and $\hat{\mathcal{N}}'_u(\cdot, \cdot; \cdot, \cdot)$ is the Jacobian of $\hat{\mathcal{N}}(\cdot, \cdot; \cdot)$ with respect to u and thus represents the discretization of $F'_u(\cdot, \cdot; \cdot)$. Further, we shall assume that (u_h, ϕ_h, λ_h) also satisfies the discrete analogue of the conditions of a pitchfork bifurcation (2.10), that is,

$$\hat{\mathcal{N}}''_{u\lambda}(u_h, \lambda_h; \phi_h, \varrho_h) + \hat{\mathcal{N}}''_{uu}(u_h, \lambda_h; w_h, \phi_h, \varrho_h) = 0, \tag{3.2}$$

where $\varrho_h \in \ker(\hat{\mathcal{N}}'_u(u_h, \lambda_h; v_h, \cdot))$ $\forall v_h$ and $w_h \in V^s_{h,p}$ is the solution to

$$\hat{\mathcal{N}}'_u(u_h, \lambda_h; w_h, \varphi_h) + \hat{\mathcal{N}}'_\lambda(u_h, \lambda_h; \varphi_h) = 0, \quad \forall \varphi_h \in V^a_{h,p}.$$

Similarly, for the Hopf bifurcation we seek to find $\mathbf{u}_{H,h} = (u_h, \phi_h, \psi_h, \lambda_h, \mu_h) \in \mathbf{V}_{H,h,p} := V^s_{h,p} \times V^a_{h,p} \times V^a_{h,p} \times \mathbb{R} \times \mathbb{R}$ such that

$$\begin{aligned}\mathcal{N}_H(\mathbf{u}_{H,h}, \mathbf{v}_h) := \hat{\mathcal{N}}(u_h, \lambda_h; v_h) + \hat{\mathcal{N}}'_u(u_h, \lambda_h; \phi_h, \varphi_h) + \mu_h(\psi_h, \varphi_h) \\ + \hat{\mathcal{N}}'_u(u_h, \lambda_h; \psi_h, \vartheta_h) - \mu_h(\phi_h, \vartheta_h) \\ + \chi_h((g, \phi_h) - 1) + \varsigma_h(g, \psi_h) = 0 \quad \forall \mathbf{v}_h \in \mathbf{V}_{H,h,p},\end{aligned} \tag{3.3}$$

where $\mathbf{v}_h = (v_h, \varphi_h, \vartheta_h, \chi_h, \varsigma_h)$.

For the proceeding error analysis we make the assumption that both (3.1) and (3.3) are consistent, that is, for the true solutions $\mathbf{u}_S$ and $\mathbf{u}_H$ of (2.9) and (2.11), respectively,

$$\mathcal{N}_S(\mathbf{u}_S, \mathbf{v}_h) = 0 \quad \forall \mathbf{v}_h \in \mathbf{V}_{S,h,p} \tag{3.4}$$

and

$$\mathcal{N}_H(\mathbf{u}_H, \mathbf{v}_h) = 0 \quad \forall \mathbf{v} \in \mathbf{V}_{H,h,p}. \tag{3.5}$$

3.1. DWR approach for functionals. For a linear target functional of practical interest $J(\cdot)$, we briefly outline the key steps involved in estimating the approximation error $J(\mathbf{u}) - J(\mathbf{u}_h)$ employing the DWR technique. We write $\mathcal{M}_*(\cdot,\cdot;\cdot,\cdot)$ to denote the mean value linearization of $\mathcal{N}_*(\cdot;\cdot)$, where $* = S, H$, respectively, defined by

$$\begin{aligned}\mathcal{M}_*(\mathbf{u}_*, \mathbf{u}_{*,h}; \mathbf{u}_* - \mathbf{u}_{*,h}, \mathbf{w}) &= \mathcal{N}_*(\mathbf{u}_*; \mathbf{w}) - \mathcal{N}_*(\mathbf{u}_{*,h}; \mathbf{w}) \\ &= \int_0^1 \mathcal{N}'_{*,\mathbf{u}}(\theta\mathbf{u}_* + (1-\theta)\mathbf{u}_{*,h}; \mathbf{u}_* - \mathbf{u}_{*,h}, \mathbf{w})\,\mathrm{d}\theta, \quad (3.6)\end{aligned}$$

for some $\mathbf{w} \in \hat{\mathbf{V}}$. Here, $\hat{\mathbf{V}}$ is some suitably chosen space such that $\mathbf{V}_{*,h,p} \subset \hat{\mathbf{V}}$, $* = S, H$. We now introduce the following (formal) *dual problem*: find $\mathbf{z}_* \in \hat{\mathbf{V}}$ such that

$$\mathcal{M}_*(\mathbf{u}_*, \mathbf{u}_{*,h}; \mathbf{w}, \mathbf{z}_*) = J(\mathbf{w}) \quad \forall \mathbf{w} \in \hat{\mathbf{V}}. \quad (3.7)$$

We assume that (3.7) possesses a unique solution. This assumption is, of course, dependent on both the definition of $\mathcal{M}_*(\mathbf{u}_*, \mathbf{u}_{*,h}; \cdot, \cdot)$ and the target functional under consideration. For the proceeding error analysis, we must therefore assume that (3.7) is well–posed. By exploiting the linearity of $J(\cdot)$, combining (3.6) and (3.7), and using the consistency condition (3.4) or (3.5) we arrive at the following error representation formula

$$\begin{aligned}J(\mathbf{u}_*) - J(\mathbf{u}_{*,h}) = J(\mathbf{u}_* - \mathbf{u}_{*,h}) &= \mathcal{M}_*(\mathbf{u}_*, \mathbf{u}_{*,h}; \mathbf{u}_* - \mathbf{u}_{*,h}, \mathbf{z}_*) \\ &= \mathcal{M}_*(\mathbf{u}_*, \mathbf{u}_{*,h}; \mathbf{u}_* - \mathbf{u}_{*,h}, \mathbf{z}_* - \mathbf{z}_{*,h}) \\ &= -\mathcal{N}_*(\mathbf{u}_{*,h}, \mathbf{z}_* - \mathbf{z}_{*,h}) \quad \forall \mathbf{z}_{*,h} \in \mathbf{V}_{*,h,p}, \quad (3.8)\end{aligned}$$

$* = S, H$. As it stands, the error representation formula (3.8) is still noncomputable since $\mathbf{z}_*$, $* = S, H$, is unknown analytically. Instead, we must seek a finite dimensional approximation $\hat{\mathbf{z}}_{*,h}$ to $\mathbf{z}_*$. Clearly, it is not possible to seek $\hat{\mathbf{z}}_{*,h} \in \mathbf{V}_{*,h,p}$, otherwise the resulting error representation would be identically zero due to (3.1) and (3.3). A number of possible alternatives exist. The first involves keeping the degree p of the approximating polynomial the same as that for $\mathbf{u}_{*,h}$, but computing $\hat{\mathbf{z}}_{*,h}$ on a sequence of dual finite element meshes $\hat{\mathcal{T}}_{\hat{h}}$ which, in general, differ from the "primal meshes" $\mathcal{T}_h$. Alternatively $\hat{\mathbf{z}}_{*,h} \in \mathbf{V}_{*,h,\hat{p}}$ may be computed using polynomials of degree $\hat{p} > p$ on the same finite element mesh $\mathcal{T}_h$ employed for the primal problem. A variant of this second approach is to compute the approximate dual solution using the same polynomial degree p as used for the primal problem and to extrapolate the resulting approximate dual solution $\hat{\mathbf{z}}_{*,h}$. Although this latter approach is the cheapest of the three methods, and is still capable of producing adaptively refined meshes specifically tailored to the selected target functional, the quality of the resulting approximate error representation formula may be poor. On the basis of numerical experimentation, we favour the second approach due to its computational simplicity of implementation.

For the purposes of this article, we are concerned in controlling the error in the computed critical bifurcation parameter and hence the target functional of interest is simply $J(\mathbf{u}_*) = \lambda$. As the dual problem involves the analytical solution $\mathbf{u}_*$ we must commit a linearization error and use the approximation $\mathbf{u}_{*,h}$ instead. Thus for a steady bifurcation, the (approximate) dual problem for estimating the error in the approximate critical parameter is defined as follows: find $\hat{\mathbf{z}}_{S,h} = (z_u, z_\phi, z_\lambda) \in \mathbf{V}_{S,h,\hat{p}}$

such that

$$\begin{aligned}\hat{\mathcal{N}}'_u(u_h,\lambda_h;v_h,z_u)+\hat{\mathcal{N}}'_\lambda(u_h,\lambda_h;z_u)\chi_h\\ +\hat{\mathcal{N}}''_{uu}(u_h,\lambda_h;\varphi_h,\phi_h,z_\phi)+\hat{\mathcal{N}}'_u(u_h,\lambda_h;\varphi_h,z_\phi)\\ +\hat{\mathcal{N}}''_{u\lambda}(u_h,\lambda_h;\phi_h,z_\phi)\chi_h+z_\lambda(g,\varphi_h)=1\quad\forall\mathbf{v}_h\in\mathbf{V}_{S,h,\hat{p}},\end{aligned}\tag{3.9}$$

where $\mathbf{v}_h=(v_h,\varphi_h,\chi_h)$. For a Hopf bifurcation the (approximate) dual problem is: find $\hat{\mathbf{z}}_{H,h}=(z_u,z_\phi,z_\psi,z_\lambda,z_\mu)\in\mathbf{V}_{H,h,\hat{p}}$ such that

$$\begin{aligned}\hat{\mathcal{N}}'_u(u_h,\lambda_h;v_h,z_u)+\hat{\mathcal{N}}'_\lambda(u_h,\lambda_h;z_u)\chi_h\\ +\hat{\mathcal{N}}''_{uu}(u_h,\lambda_h;\varphi_h,\phi_h,z_\phi)+\hat{\mathcal{N}}'_u(u_h,\lambda_h;\varphi_h,z_\phi)\\ +\mu_h(\theta_h,z_\phi)+\varsigma_h(\psi_h,z_\phi)+\hat{\mathcal{N}}''_{u\lambda}(u_h,\lambda_h;\phi_h,z_\phi)\chi_h\\ +\hat{\mathcal{N}}''_{uu}(u_h,\lambda_h;\theta_h,\psi_h,z_\psi)+\hat{\mathcal{N}}'_u(u_h,\lambda_h;\theta_h,z_\psi)\\ -\mu_h(\varphi_h,z_\psi)-\varsigma_h(\phi_h,z_\psi)+\hat{\mathcal{N}}''_{u\lambda}(u_h,\lambda_h;\psi_h,z_\psi)\chi_h\\ +z_\lambda(g,\varphi_h)+z_\mu(g,\theta_h)=1\quad\forall\mathbf{v}_h\in\mathbf{V}_{H,h,\hat{p}},\end{aligned}\tag{3.10}$$

where $\mathbf{v}_h=(v_h,\varphi_h,\theta_h,\chi_h,\varsigma_h)$.

4. Solution procedure. In this section we outline how the primal and dual problems may be solved in an efficient manner by reducing the extended systems to a succession of smaller matrix problems.

4.1. Steady bifurcation. To determine the numerical solution $\mathbf{u}_{S,h}$ to the nonlinear system of equations (3.1), we employ a damped Newton method. This nonlinear iteration generates a sequence of approximations $\mathbf{u}^n_{S,h}$, $n=1,2,\ldots$, to the actual numerical solution $\mathbf{u}_{S,h}$ using the following algorithm. Given an iterate $\mathbf{u}^n_{S,h}$, the update $\mathbf{d}^n_h:=(du^n_h,d\phi^n_h,d\lambda^n_h,)$ to $\mathbf{u}^n_{S,h}$ to get to the next iterate

$$\mathbf{u}^{n+1}_{S,h}=\mathbf{u}^n_{S,h}+\omega^n\mathbf{d}^n_h$$

is defined by: find $\mathbf{d}^n_h$ such that for all $\mathbf{v}_h=(v_h,\varphi_h,\chi_h)\in\mathbf{V}_{S,h,p}$

$$\begin{aligned}\hat{\mathcal{N}}'_u(u^n_h,\lambda^n_h;du^n_h,v_h)+\hat{\mathcal{N}}'_\lambda(u^n_h,\lambda^n_h;v_h)d\lambda^n_h=r^n_1(v_h),\\ \hat{\mathcal{N}}''_{uu}(u^n_h,\lambda^n_h;du^n_h,\phi^n_h,\varphi_h)\\ +\hat{\mathcal{N}}'_u(u^n_h,\lambda^n_h;d\phi^n_h,\varphi_h)+\hat{\mathcal{N}}''_{u\lambda}(u^n_h,\lambda^n_h;\phi^n_h,\varphi_h)d\lambda^n_h=r^n_2(\varphi_h),\\ \chi_h(d\phi^n_h,c)=r^n_3(\chi_h).\end{aligned}\tag{4.1}$$

Here, $r^n_1(\cdot)$, $r^n_2(\cdot)$ and $r^n_3(\cdot)$ are residuals given, respectively, by

$$r^n_1(v_h)=-\hat{\mathcal{N}}(u^n_h,\lambda^n_h;v_h),\ r^n_2(\varphi_h)=-\hat{\mathcal{N}}'_u(u^n_h,\lambda^n_h;\phi^n_h,\varphi_h),$$

$$r^n_3(\chi_h)=-\chi_h((\phi^n_h,g)-1).$$

If the spaces $V^s_{h,p}$ and $V^a_{h,p}$ are both of dimension N (which need not be the case), then the problem (4.1) is of size $2N+1$, which will be extremely large for the fluid flow problems considered in the forthcoming sections. Instead, we carry out an LU-decomposition of the matrices arising in the Newton iteration in order to reduce the problem to a succession of smaller matrix problems. Assuming a Galerkin type approximation of $\mathbf{u}_{S,h}$ is exploited, in which case $u^n_h=\sum_{i=1}^N U^n_i\varphi_i$, $\phi^n_h=\sum_{i=1}^N\Phi^n_i\zeta_i$,

where $\{\varphi_i\}_{i=1}^N$ is a basis for $V_{h,p}^s$ and $\{\zeta_i\}_{i=1}^N$ is a basis for $V_{h,p}^a$. Similarly, we let $du_h^n = \sum_{i=1}^N dU_i^n \varphi_i$ and $d\phi_h^n = \sum_{i=1}^N d\Phi_i^n \zeta_i$. For ease of exposition we define $\boldsymbol{\phi}_h^n = \{\Phi_i^n\}_{i=1}^N$, $\boldsymbol{d}u_h^n = \{dU_i^n\}_{i=1}^N$ and $\boldsymbol{d}\phi_h^n = \{d\Phi_i^n\}_{i=1}^N$ and with an abuse of notation, we may rewrite (4.1) in the following form

$$\begin{bmatrix} \mathrm{F}_u^{s,n} & 0 & \boldsymbol{F}_\lambda^{s,n} \\ \mathrm{F}_{uu}^{a,n} & \mathrm{F}_u^{a,n} & \boldsymbol{F}_{u\lambda}^{a,n} \\ \mathbf{0}^\top & \boldsymbol{l}^\top & 0 \end{bmatrix} \begin{bmatrix} \boldsymbol{d}u_h^n \\ \boldsymbol{d}\boldsymbol{\phi}_h^n \\ d\lambda_h^n \end{bmatrix} = \begin{bmatrix} \boldsymbol{r}_1^n \\ \boldsymbol{r}_2^n \\ r_3^n \end{bmatrix}. \tag{4.2}$$

Here, the matrices $\mathrm{F}_u^{s,n}$, $\mathrm{F}_u^{a,n}$ and $\mathrm{F}_{uu}^{a.n}$ are given, respectively, by

$$\{\mathrm{F}_u^{s,n}\}_{i,j=1}^N = \{\hat{\mathcal{N}}_u'(u_h^n, \lambda_h^n; \varphi_i, \varphi_j)\}_{i,j=1}^N,$$

$$\{\mathrm{F}_u^{a,n}\}_{i,j=1}^N = \{\hat{\mathcal{N}}_u'(u_h^n, \lambda_h^n; \zeta_i, \zeta_j)\}_{i,j=1}^N,$$

$$\{\mathrm{F}_{uu}^{a.n}\}_{i,j=1}^N = \{\hat{\mathcal{N}}_{uu}''(u_h^n, \lambda_h^n; \varphi_i, \phi_h^n, \zeta_j)\}_{i,j=1}^N,$$

and the vectors $\boldsymbol{F}_\lambda^{s,n}$, $\boldsymbol{F}_{u\lambda}^{a,n}$ and $\boldsymbol{l}$ are defined, respectively, by

$$\{\boldsymbol{F}_\lambda^{s,n}\}_{i=1}^N = \{\hat{\mathcal{N}}_\lambda'(u_h^n, \lambda_h^n; \varphi_i)\}_{i=1}^N,$$

$$\{\boldsymbol{F}_{u\lambda}^{a,n}\}_{i=1}^N = \{\hat{\mathcal{N}}_{u\lambda}''(u_h^n, \lambda_h^n; \phi_h^n, \zeta_i)\}_{i=1}^N,$$

$$\{\boldsymbol{l}\}_{i=1}^N = \{(c, \zeta_i)\}_{i=1}^N.$$

Finally, the residual vectors $\boldsymbol{r}_1^n$ and $\boldsymbol{r}_2^n$ are given, respectively, by

$$\{\boldsymbol{r}_1^n\}_{i=1}^N = \{r_1^n(\varphi_i)\}_{i=1}^N \quad \text{and} \quad \{\boldsymbol{r}_2^n\}_{i=1}^N = \{r_2^n(\zeta_i)\}_{i=1}^N;$$

recall that $r_3^n(\chi_h) = -\chi_h((\phi_h^n, g) - 1)$. The matrix appearing in (4.2) can then be written in block LU format as:

$$\begin{bmatrix} \mathrm{F}_u^{s,n} & 0 & \boldsymbol{F}_\lambda^{s,n} \\ \mathrm{F}_{uu}^{a,n} & \mathrm{F}_u^{a,n} & \boldsymbol{F}_{u\lambda}^{a,n} \\ \mathbf{0}^\top & \boldsymbol{l}^\top & 0 \end{bmatrix} = \mathrm{LU}, \tag{4.3}$$

where

$$\mathrm{L} = \left[\begin{array}{c|cc} \mathrm{F}_u^{s,n} & 0 & \mathbf{0} \\ \hline \mathrm{F}_{uu}^{a,n} & \mathrm{I} & \mathbf{0} \\ \mathbf{0}^\top & \mathbf{0}^\top & 1 \end{array}\right] \text{ and } \mathrm{U} = \left[\begin{array}{c|cc} \mathrm{I} & 0 & -\boldsymbol{w}^{s,n} \\ \hline 0 & \mathrm{F}_u^{a,n} & \mathrm{F}_{uu}^{a,n}\boldsymbol{w}^{s,n} + \boldsymbol{F}_{u\lambda}^{a,n} \\ \mathbf{0}^\top & \boldsymbol{l}^\top & 0 \end{array}\right],$$

and $\boldsymbol{w}^{s,n}$ satisfies

$$\mathrm{F}_u^{s,n}\boldsymbol{w}^{s,n} = -\boldsymbol{F}_\lambda^{s,n}. \tag{4.4}$$

The foregoing assumptions guarantee that, at the bifurcation point, both F_u^s and the matrix

$$\begin{bmatrix} \mathrm{F}_u^{a,n} & \mathrm{F}_{uu}^{a,n}\boldsymbol{w}^{s,n} + \boldsymbol{F}_{u\lambda}^{a,n} \\ \boldsymbol{l}^\top & 0 \end{bmatrix}, \tag{4.5}$$

evaluated at (u_h, λ_h), are nonsingular. This follows immediately upon application of Lemma 2.2 along with (3.2). Thus, a continuity argument ensures that for $(u_h^n, \phi_h^n, \lambda_h^n)$ sufficiently close to (u_h, ϕ_h, λ_h) equation (4.2) is soluble. In particular, at each Newton iteration, the solution to the $(2N+1) \times (2N+1)$ matrix problem (4.2) may be computed based on solving two $N \times N$ matrix problems involving $\mathrm{F}_u^{s,n}$, and one $(N+1) \times (N+1)$ matrix problem involving (4.5), together with appropriate forward and backward substitutions. We point out that the first linear solve involving the matrix $\mathrm{F}_u^{s,n}$ is necessary to first compute the vector $\boldsymbol{w}^{s,n}$, cf. (4.4) above, while the second solve is undertaken in the forward substitution employing the matrix L. In order that the Newton iteration converges, we must have a good initial guess for both the steady state solution and the nullfunction. This is achieved based on employing the following continuation procedure: the steady solution and most dangerous eigenvalue are first computed for a small value of the critical parameter. The critical parameter is then gradually increased until there is a change in sign of the real part of the left most eigenvalue; when this occurs the computed base solution/eigenfunction pair is then taken as the initial guess for the Newton iteration.

To solve the approximate dual problem for the steady bifurcation, we first write $z_u = \sum_{i=1}^{\hat{N}} Z_{u,i}\hat{\varphi}_i$, $z_\phi = \sum_{i=1}^{\hat{N}} Z_{\phi,i}\hat{\zeta}_i$, $\boldsymbol{z}_u = \{Z_{u,i}\}_{i=1}^{\hat{N}}$, and $\boldsymbol{z}_\phi = \{Z_{\phi,i}\}_{i=1}^{\hat{N}}$, where $\{\hat{\varphi}_i\}_{i=1}^{\hat{N}}$ and $\{\hat{\zeta}_i\}_{i=1}^{\hat{N}}$ denote a suitable set of linearly independent finite element basis functions which span $V_{h,\hat{p}}^s$ and $V_{h,\hat{p}}^a$, respectively. Thus, we can rewrite the dual problem (3.9) as: find the triple $(\boldsymbol{z}_u, \boldsymbol{z}_\phi, z_\lambda)$ satisfying

$$\begin{bmatrix} (\hat{\mathrm{F}}_u^s)^\top & (\hat{\mathrm{F}}_{uu}^a)^\top & \mathbf{0} \\ 0 & (\hat{\mathrm{F}}_u^a)^\top & \hat{\boldsymbol{l}} \\ (\hat{\boldsymbol{F}}_\lambda^s)^\top & (\hat{\boldsymbol{F}}_{u\lambda}^a)^\top & 0 \end{bmatrix} \begin{bmatrix} \boldsymbol{z}_u \\ \boldsymbol{z}_\phi \\ z_\lambda \end{bmatrix} = \begin{bmatrix} \mathbf{0} \\ \mathbf{0} \\ 1 \end{bmatrix}. \tag{4.6}$$

Here, $\hat{\mathrm{F}}_u^s$ is understood to be the Jacobian on the space $V_{h,\hat{p}}^s$ evaluated at u_h, and so on. Hence, the matrix involved in the computation of the dual solution is no more than the transpose of that used in the Newton solves, albeit defined on a larger finite dimensional space. Thus, we can use the same LU decomposition proposed above to reduce the computational complexity involved in evaluating the solution of this problem.

4.2. Hopf bifurcation. In a process very similar to that for the steady bifurcation, for a Hopf bifurcation we find a sequence of approximations $\mathbf{u}_{H,h}^n$, $n = 1, 2, \ldots$ to the solution of (3.3) using a damped Newton method. Thus, given an iterate $\mathbf{u}_{H,h}^n$, the update $\mathbf{d}_h^n = (du_h^n, d\phi_h^n, d\psi_h^n, d\lambda_h^n, d\mu_h^n)$ is found by solving

$$\begin{aligned}
\hat{\mathcal{N}}_u'(u_h^n, \lambda_h^n; du_h^n, v_h) + \hat{\mathcal{N}}_\lambda'(u_h^n, \lambda_h^n; v_h) d\lambda_h^n &= r_1^n(v_h), \\
\hat{\mathcal{N}}_{uu}''(u_h^n, \lambda_h^n; du_h^n, \phi_h^n, \varphi_h) & \\
+ \hat{\mathcal{N}}_u'(u_h^n, \lambda_h^n; d\phi_h^n, \varphi_h) + \hat{\mathcal{N}}_{u\lambda}''(u_h^n, \lambda_h^n; \phi_h^n, \varphi_h) d\lambda_h^n & \\
+ \mu_h^n(d\psi_h^n, \varphi_h) + d\mu_h^n(\psi_h^n, \varphi_h) &= r_2^n(\varphi_h), \\
\hat{\mathcal{N}}_{uu}''(u_h^n, \lambda_h^n; du_h^n, \psi_h^n, \theta_h) & \\
+ \hat{\mathcal{N}}_u'(u_h^n, \lambda_h^n; d\psi_h^n, \theta_h) + \hat{\mathcal{N}}_{u\lambda}''(u_h^n, \lambda_h^n; \psi_h^n, \theta_h) d\lambda_h^n & \\
- \mu_h^n(d\phi_h^n, \theta_h) - d\mu_h^n(\phi_h^n, \theta_h) &= r_3^n(\theta_h), \\
\chi_h(d\phi_h^n, g) &= r_4^n(\chi_h), \\
\varsigma_h(d\psi_h^n, g) &= r_5^n(\varsigma_h).
\end{aligned} \tag{4.7}$$

Here, $r_1^n(\cdot), \ldots, r_5^n(\cdot)$ are residuals given, respectively, by

$$r_1^n(v_h) = -\hat{\mathcal{N}}(u_h^n, \lambda_h^n; v_h),\ r_2^n(\varphi_h) = -\hat{\mathcal{N}}'_u(u_h^n, \lambda_h^n; \phi_h^n, \varphi_h) - \mu_h^n(\psi_h^n, \varphi_h),$$

$$r_3^n(\theta_h) = -\hat{\mathcal{N}}'_u(u_h^n, \lambda_h^n; \psi_h^n, \varphi_h) + \mu_h^n(\phi_h^n, \theta_h),$$

$$r_4^n(\chi_h) = -\chi_h((\phi_h^n, g) - 1),\ r_5^n = -\varsigma_h(\psi_h^n, g).$$

Once again, assuming a Galerkin type approximation of $\mathbf{u}_{H,h}$ is exploited, we may write $u_h^n = \sum_{i=1}^N U_i^n \varphi_i$, $\phi_h^n = \sum_{i=1}^N \Phi_i^n \zeta_i$, and $\psi_h^n = \sum_{i=1}^N \Psi_i^n \zeta_i$, where $\{\varphi_i\}_{i=1}^N$ is a basis for $V_{h,p}^s$ and $\{\zeta_i\}_{i=1}^N$ is a basis for $V_{h,p}^a$. Similarly, we let $du_h^n = \sum_{i=1}^N dU_i^n \varphi_i$, $d\phi_h^n = \sum_{i=1}^N d\Phi_i^n \zeta_i$ and $d\psi_h^n = \sum_{i=1}^N d\Psi_i^n \zeta_i$. Again, for ease of exposition we define $\boldsymbol{\phi}_h^n = \{\Phi_i\}_{i=1}^N$, $\boldsymbol{\psi}_h^n = \{\Psi_i\}_{i=1}^N$, $\boldsymbol{du}_h^n = \{dU_i^n\}_{i=1}^N$, $\boldsymbol{d\phi}_h^n = \{d\Phi_i^n\}_{i=1}^N$ and $\boldsymbol{d\psi}_h^n = \{d\Psi_i^n\}_{i=1}^N$. As in the case of the steady bifurcation, with a slight abuse of notation, (4.7) can be rewritten in the form

$$\begin{bmatrix} \mathrm{F}_u^{s,n} & 0 & 0 & \boldsymbol{F}_\lambda^{s,n} & 0 \\ \mathrm{F}_{uu}^{\phi,n} & \mathrm{F}_u^{a,n} & \mu_h^n \mathrm{M} & \boldsymbol{F}_{u\lambda}^{\phi,n} & \mathrm{M}\boldsymbol{\psi}_h^n \\ \mathrm{F}_{uu}^{\psi,n} & -\mu_h^n \mathrm{M} & \mathrm{F}_u^{a,n} & \boldsymbol{F}_{u\lambda}^{\psi,n} & -\mathrm{M}\boldsymbol{\phi}_h^n \\ \mathbf{0}^\top & \boldsymbol{l}^\top & \mathbf{0}^\top & 0 & 0 \\ \mathbf{0}^\top & \mathbf{0}^\top & \boldsymbol{l}^\top & 0 & 0 \end{bmatrix} \begin{bmatrix} \boldsymbol{du}_h^n \\ \boldsymbol{d\phi}_h^n \\ \boldsymbol{d\psi}_h^n \\ d\lambda_h^n \\ d\mu_h^n \end{bmatrix} = \begin{bmatrix} \boldsymbol{r}_1^n \\ \boldsymbol{r}_2^n \\ \boldsymbol{r}_3^n \\ r_4^n \\ r_5^n \end{bmatrix}. \tag{4.8}$$

Here, the matrices $\mathrm{F}_u^{s,n}$ and $\mathrm{F}_u^{a,n}$ and the vectors $\boldsymbol{F}_\lambda^{s,n}$, $\boldsymbol{l}$ and $\boldsymbol{r}_1$ are defined analogously as for the steady bifurcation problem. Moreover, $\mathrm{F}_{uu}^{\phi,n}$ and $\mathrm{F}_{uu}^{\psi,n}$ are given, respectively, by

$$\{\mathrm{F}_{uu}^{\phi,n}\}_{i,j=1}^N = \{\hat{\mathcal{N}}''_{uu}(u_h^n, \lambda_h^n; \varphi_i, \phi_h^n, \zeta_j)\}_{i,j=1}^N,$$

$$\{\mathrm{F}_{uu}^{\psi,n}\}_{i,j=1}^N = \{\hat{\mathcal{N}}''_{uu}(u_h^n, \lambda_h^n; \varphi_i, \psi_h^n, \zeta_j)\}_{i,j=1}^N,$$

and the vectors $\boldsymbol{F}_{u\lambda}^{\phi,n}$ and $\boldsymbol{F}_{u\lambda}^{\psi,n}$ are defined, respectively, by

$$\{\boldsymbol{F}_{u\lambda}^{\phi,n}\}_{i=1}^N = \{\hat{\mathcal{N}}''_{u\lambda}(u_h^n, \lambda_h^n; \phi_h^n, \zeta_i)_{i=1}^N,$$

$$\{\boldsymbol{F}_{u\lambda}^{\psi,n}\}_{i=1}^N = \{\hat{\mathcal{N}}''_{u\lambda}(u_h^n, \lambda_h^n; \psi_h^n, \zeta_i)_{i=1}^N.$$

Finally, M is the mass matrix given by

$$\{\mathrm{M}\}_{i,j=1}^N = \{(\zeta_i, \zeta_j)\}_{i,j=1}^N,$$

and $\boldsymbol{r}_2$ and $\boldsymbol{r}_3$ are the residual vectors defined, respectively, by

$$\{\boldsymbol{r}_2\}_{i=1}^N = \{r_2(\zeta_i)\}_{i=1}^N \text{ and } \{\boldsymbol{r}_3\}_{i=1}^N = \{r_3(\zeta_i)\}_{i=1}^N.$$

A block LU decomposition of the matrix arising in (4.8) yields

$$\begin{bmatrix} \mathrm{F}_u^{s,n} & 0 & 0 & \boldsymbol{F}_\lambda^{s,n} & 0 \\ \mathrm{F}_{uu}^{\phi,n} & \mathrm{F}_u^{a,n} & \mu_h^n \mathrm{M} & \boldsymbol{F}_{u\lambda}^{\phi,n} & \mathrm{M}\boldsymbol{\psi}_h^n \\ \mathrm{F}_{uu}^{\psi,n} & -\mu_h^n \mathrm{M} & \mathrm{F}_u^{a,n} & \boldsymbol{F}_{u\lambda}^{\psi,n} & -\mathrm{M}\boldsymbol{\phi}_h^n \\ \mathbf{0}^\top & \boldsymbol{l}^\top & \mathbf{0}^\top & 0 & 0 \\ \mathbf{0}^\top & \mathbf{0}^\top & \boldsymbol{l}^\top & 0 & 0 \end{bmatrix} = \mathrm{LU}, \tag{4.9}$$

where

$$\mathrm{L} = \left[\begin{array}{c|cccc} \mathrm{F}_u^{s,n} & 0 & 0 & \mathbf{0} & \mathbf{0} \\ \hline \mathrm{F}_{uu}^{\phi,n} & \mathrm{I} & 0 & \mathbf{0} & \mathbf{0} \\ \mathrm{F}_{uu}^{\psi,n} & 0 & \mathrm{I} & \mathbf{0} & \mathbf{0} \\ \mathbf{0}^\top & \mathbf{0}^\top & \mathbf{0}^\top & 1 & 0 \\ \mathbf{0}^\top & \mathbf{0}^\top & \mathbf{0}^\top & 0 & 1 \end{array}\right]$$

and

$$\mathrm{U} = \left[\begin{array}{c|cc|cc} \mathrm{I} & 0 & 0 & -\boldsymbol{w}^{s,n} & \mathbf{0} \\ \hline 0 & \mathrm{F}_u^{a,n} & \mu_h^n \mathrm{M} & \mathrm{F}_{uu}^{\phi,n}\boldsymbol{w}^{s,n} + \boldsymbol{F}_{u\lambda}^{\phi,n} & \mathrm{M}\boldsymbol{\psi}_h^n \\ 0 & -\mu_h^n \mathrm{M} & \mathrm{F}_u^{a,n} & \mathrm{F}_{uu}^{\psi,n}\boldsymbol{w}^{s,n} + \boldsymbol{F}_{u\lambda}^{\psi,n} & -\mathrm{M}\boldsymbol{\phi}_h^n \\ \mathbf{0}^\top & \boldsymbol{l}^\top & \mathbf{0}^\top & 0 & 0 \\ \mathbf{0}^\top & \mathbf{0}^\top & \boldsymbol{l}^\top & 0 & 0 \end{array}\right];$$

again $\boldsymbol{w}^{s,n}$ satisfies $\mathrm{F}_u^{s,n}\boldsymbol{w}^{s,n} = -\boldsymbol{F}_\lambda^{s,n}$. Under the assumption that both $V_{h,p}^s$ and $V_{h,p}^a$ are of dimension N, the overall size of the underlying matrix stemming from the discretization of the Hopf bifurcation problem is $3N+2$. By exploiting the LU-decomposition in (4.9) the solution to (4.8) can be computed based on solving two $N \times N$ matrix problems involving $\mathrm{F}_u^{s,n}$, and one $(2N+2)\times(2N+2)$ matrix problem, together with appropriate forward and backward substitutions.

Writing $z_u = \sum_{i=1}^{\hat{N}} Z_{u,i}\hat{\varphi}_i$, $z_\phi = \sum_{i=1}^{\hat{N}} Z_{\phi,i}\hat{\zeta}_i$, $z_\psi = \sum_{i=1}^{\hat{N}} Z_{\psi,i}\hat{\zeta}_i$ $\boldsymbol{z}_u = \{Z_{u,i}\}_{i=1}^{\hat{N}}$, $\boldsymbol{z}_\phi = \{Z_{\phi,i}\}_{i=1}^{\hat{N}}$ and $\boldsymbol{z}_\psi = \{Z_{\psi,i}\}_{i=1}^{\hat{N}}$, where again $\{\hat{\varphi}_i\}_{i=1}^{\hat{N}}$ and $\{\hat{\zeta}_i\}_{i=1}^{\hat{N}}$ denote a suitable set of linearly independent finite element basis functions which span $V_{h,\hat{p}}^s$ and $V_{h,\hat{p}}^a$, respectively, the associated dual problem for the error estimation of the critical parameter when a Hopf bifurcation occurs can be written in the following form

$$\left[\begin{array}{ccccc} (\hat{\mathrm{F}}_u^s)^\top & (\hat{\mathrm{F}}_{uu}^\phi)^\top & (\hat{\mathrm{F}}_{uu}^\psi)^\top & \mathbf{0} & \mathbf{0} \\ 0 & (\hat{\mathrm{F}}_u^a)^\top & -\mu_h \mathrm{M}^\top & \hat{\boldsymbol{l}} & \mathbf{0} \\ 0 & \mu_h \mathrm{M}^\top & (\hat{\mathrm{F}}_u^a)^\top & \mathbf{0} & \hat{\boldsymbol{l}} \\ (\hat{\boldsymbol{F}}_\lambda^s)^\top & (\hat{\boldsymbol{F}}_{u\lambda}^\phi)^\top & (\hat{\boldsymbol{F}}_{u\lambda}^\psi)^\top & 0 & 0 \\ 0 & (\mathrm{M}\boldsymbol{\psi}_h)^\top & -(\mathrm{M}\boldsymbol{\phi}_h)^\top & 0 & 0 \end{array}\right] \left[\begin{array}{c} \boldsymbol{z}_u \\ \boldsymbol{z}_\phi \\ \boldsymbol{z}_\psi \\ z_\lambda \\ z_\mu \end{array}\right] = \left[\begin{array}{c} \mathbf{0} \\ \mathbf{0} \\ \mathbf{0} \\ 1 \\ 0 \end{array}\right], \tag{4.10}$$

where again $\hat{\mathrm{F}}_u^s$ is understood to be the Jacobian evaluated on the space $V_{h,\hat{p}}^s$, and so on. As before, the same LU decomposition proposed in (4.9) can be used to reduce the complexity involved in evaluating the solution of this problem.

5. Problem specification and discontinuous Galerkin discretization. In this section we outline the application of the above theory to the problem of incompressible fluid flow in an open system whose geometry has reflectional symmetry about one and only one axis. In particular, for the discretization of the underlying bifurcation problem, we exploit the symmetric version of the interior penalty DG method.

5.1. Incompressible Navier-Stokes equations. Consider the flow of an incompressible fluid confined in a generic two-dimensional channel $\Omega \in \mathbb{R}^2$ of width D, with boundary $\Gamma = \Gamma_{\mathrm{D}} \cup \Gamma_{\mathrm{N}}$. Additionally, we write Γ_{M} to denote an axis of reflectional symmetry, lying on the x-axis. A simple example of such a geometry is depicted in Figure 5.1, though we point out that the proceeding discussion holds for more general computational domains. On Γ_{D} we impose a Dirichlet boundary condition, while on Γ_{N} a natural Neumann condition is enforced. By introducing the

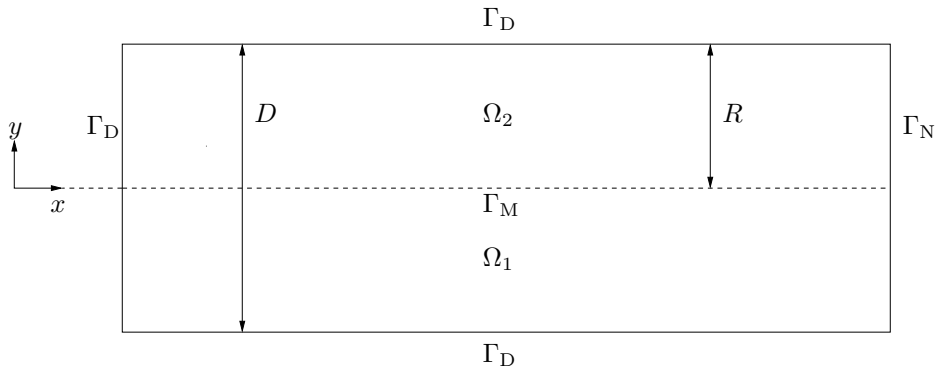

FIG. 5.1. *Generic channel domain* $\Omega = \Omega_1 \cup \Omega_2$.

Reynolds number Re, defined as $Re = Ru_{\max}/\nu$, where $R = D/2$ is the half width of the channel, $u_{\max}$ is the peak inlet velocity and ν is the kinematic viscosity, the flow can be modelled by the following non-dimensionalized unsteady Navier-Stokes equations: find $\mathbf{u} = [u_x, u_y]^\top$ and p such that

$$\frac{\partial \mathbf{u}}{\partial t} - \frac{1}{Re}\nabla^2 \mathbf{u} + (\mathbf{u}\cdot\nabla)\mathbf{u} + \nabla p = \mathbf{0}, \quad \text{in } \Omega, \tag{5.1}$$

$$\nabla \cdot \mathbf{u} = 0, \quad \text{in } \Omega, \tag{5.2}$$

with boundary conditions

$$\mathbf{u} = \mathbf{g}_{\mathrm{D}} \quad \text{on } \Gamma_{\mathrm{D}}, \tag{5.3}$$

and

$$\frac{1}{Re}\frac{\partial \mathbf{u}}{\partial \mathbf{n}} - p\mathbf{n} = 0 \quad \text{on } \Gamma_{\mathrm{N}}, \tag{5.4}$$

subject to some appropriate initial condition. Here, $\mathbf{u}$ and p denote the velocity and pressure of the fluid, respectively, and $\mathbf{n} = (n_x, n_y)^\top$ denotes the unit outward normal vector to the boundary Γ of Ω. In the sequel we consider the numerical approximation of the corresponding steady state problem and investigate its linear stability. With this in mind, employing the continuity equation (5.2), we rewrite the steady Navier–Stokes equations in the following divergence form (to facilitate the DG discretization): find $\mathbf{u}^0$ and p^0 such that

$$-\frac{1}{Re}\nabla^2 \mathbf{u}^0 + \nabla\cdot(\mathbf{u}^0 \otimes \mathbf{u}^0) + \nabla p^0 = \mathbf{0}, \quad \text{in } \Omega, \tag{5.5}$$

$$\nabla \cdot \mathbf{u}^0 = 0, \quad \text{in } \Omega, \tag{5.6}$$

subject to the boundary conditions outlined in (5.3)–(5.4) above, with $\mathbf{u}$ and p replaced by $\mathbf{u}^0$ and p^0, respectively. Here, for vectors $\mathbf{v} \in \mathbb{R}^m$ and $\mathbf{w} \in \mathbb{R}^n$, $m, n \geq 1$, the matrix $\mathbf{v}\otimes\mathbf{w} \in \mathbb{R}^{m\times n}$ is the standard outer product defined by $(\mathbf{v}\otimes\mathbf{w})_{kl} = v_k w_l$. For ease of exposition we define the flux $\mathcal{F}^0(\cdot)$ as

$$\mathcal{F}^0(\mathbf{u}^0) := \mathbf{u}^0 \otimes \mathbf{u}^0.$$

Equations (5.5)–(5.6) may be combined to define a mapping $F : V \times \mathbb{R} \to V$, where $V = H^1(\Omega)^2 \times L^2(\Omega)$. Moreover, the bounded linear operator

$$\rho_s \begin{pmatrix} u_x(x,y) \\ u_y(x,y) \\ p(x,y) \end{pmatrix} = \begin{pmatrix} u_x(x,-y) \\ -u_y(x,-y) \\ p(x,-y) \end{pmatrix}$$

is a representation of the symmetry group Z_2 on the Hilbert space V. It is straightforward to show that the operator F is equivariant with respect to ρ_s. Applying the theory developed in Section 2.1, the solution space V admits the decomposition $V = V^s \oplus V^a$. Hence, a solution $(\mathbf{u}^0, p^0) \in V^s$ can be found by reducing the domain to either Ω_i, $i = 1, 2$, and solving: find $\mathbf{u}^0$ and p^0 such that

$$\mathcal{L}^0(\mathbf{u}^0, Re; p^0) \equiv -\frac{1}{Re}\nabla^2\mathbf{u}^0 + \nabla\cdot(\mathbf{u}^0 \otimes \mathbf{u}^0) + \nabla p^0 = \mathbf{0}, \quad \text{in } \Omega_i, \tag{5.7}$$

$$\nabla\cdot\mathbf{u}^0 = 0, \quad \text{in } \Omega_i, \tag{5.8}$$

with boundary conditions

$$\mathbf{u}^0 = \mathbf{g}_{\mathrm{D}} \quad \text{on } \Gamma_{\mathrm{D}}, \tag{5.9}$$

$$\frac{1}{Re}\frac{\partial\mathbf{u}^0}{\partial\mathbf{n}} - p^0\mathbf{n} = 0 \quad \text{on } \Gamma_{\mathrm{N}}, \tag{5.10}$$

$$\frac{1}{Re}\frac{\partial u_x^0}{\partial\mathbf{n}} - p^0 n_x = 0 \quad \text{and} \quad u_y^0 = 0 \quad \text{on } \Gamma_{\mathrm{M}}. \tag{5.11}$$

Without loss of generality, we assume from now on that we solve on the domain Ω_1. Upon linearization of the unsteady Navier–Stokes equations (5.1)–(5.2), we obtain the following eigenvalue problem for the pair $\{\lambda^m, (\mathbf{u}^m, p^m)\}$:

$$\mathcal{L}^m(\mathbf{u}^0, Re; \mathbf{u}^m, p^m) \equiv -\frac{1}{Re}\nabla^2\mathbf{u}^m + \nabla\cdot(\mathbf{u}^m \otimes \mathbf{u}^0) + \nabla\cdot(\mathbf{u}^0 \otimes \mathbf{u}^m) + \nabla p^m = \lambda^m\mathbf{u}^m, \quad \text{in } \Omega, \tag{5.12}$$

$$-\nabla\cdot\mathbf{u}^m = 0, \quad \text{in } \Omega, \tag{5.13}$$

subject to the homogeneous Dirichlet and Neumann conditions

$$\mathbf{u}^m = 0 \quad \text{on } \Gamma_{\mathrm{D}}, \tag{5.14}$$

$$\frac{1}{Re}\frac{\partial\mathbf{u}^m}{\partial\mathbf{n}} - p^m\mathbf{n} = 0 \quad \text{on } \Gamma_{\mathrm{N}}. \tag{5.15}$$

Assuming that $(\mathbf{u}^0, p^0) \in V^s$, exploiting Corollary 2.4 in the case of only seeking anti-symmetric eigenfunctions, we can reduce (5.12)–(5.15) to finding $\{\lambda^a, (\mathbf{u}^a, p^a)\} \in \mathbb{C} \times V^a$ such that

$$\mathcal{L}^a(\mathbf{u}^0, Re; \mathbf{u}^a, p^a) \equiv -\frac{1}{Re}\nabla^2\mathbf{u}^a + \nabla\cdot(\mathbf{u}^a \otimes \mathbf{u}^0) + \nabla\cdot(\mathbf{u}^0 \otimes \mathbf{u}^a) + \nabla p^a = \lambda^a\mathbf{u}^a, \quad \text{in } \Omega_1, \tag{5.16}$$

$$-\nabla\cdot\mathbf{u}^a = 0, \quad \text{in } \Omega_1, \tag{5.17}$$

subject to the homogeneous Dirichlet and Neumann conditions

$$\mathbf{u}^a = 0 \quad \text{on } \Gamma_{\mathrm{D}}, \tag{5.18}$$

$$\frac{1}{Re}\frac{\partial \mathbf{u}^a}{\partial \mathbf{n}} - p^a \mathbf{n} = 0 \quad \text{on } \Gamma_{\mathrm{N}}, \tag{5.19}$$

$$u_x^a = 0 \quad \text{and} \quad \frac{1}{Re}\frac{\partial u_y^a}{\partial \mathbf{n}} - p^a n_y = 0 \quad \text{on } \Gamma_{\mathrm{M}}. \tag{5.20}$$

Thus, to determine the Reynolds number at which a steady symmetry breaking bifurcation occurs we solve the following extended system: find $\mathbf{u}_S = \{(\mathbf{u}^0, p^0), (\mathbf{u}^a, p^a), Re^0\} \in V^s \times V^a \times \mathbb{R}$ such that

$$\begin{pmatrix} \mathcal{L}^0(\mathbf{u}^0, Re^0; p^0) \\ \nabla \cdot \mathbf{u}^0 \\ \mathcal{L}^a(\mathbf{u}^0, Re^0; \mathbf{u}^a, p^a) \\ \nabla \cdot \mathbf{u}^a \\ (\mathbf{u}^a, g) - 1 \end{pmatrix} = \mathbf{0}, \tag{5.21}$$

subject to the boundary conditions (5.9)–(5.11) and (5.18)–(5.20).

Similarly, for a symmetry breaking Hopf bifurcation we seek to computed $\mathbf{u}_H = \{(\mathbf{u}^0, p^0), (\mathbf{u}^a, p^a), (\tilde{\mathbf{u}}^a, \tilde{p}^a), Re^0, \mu^a\} \in V^s \times V^a \times V^a \times \mathbb{R} \times \mathbb{R}$ such that

$$\begin{pmatrix} \mathcal{L}^0(\mathbf{u}^0, Re^0; p^0) \\ \nabla \cdot \mathbf{u}^0 \\ \mathcal{L}^a(\mathbf{u}^0, Re^0; \mathbf{u}^a, p^a) + \mu^a \tilde{\mathbf{u}}^a \\ \nabla \cdot \mathbf{u}^a \\ \mathcal{L}^a(\mathbf{u}^0, Re^0; \tilde{\mathbf{u}}^a, \tilde{p}^a) - \mu^a \mathbf{u}^a \\ \nabla \cdot \tilde{\mathbf{u}}^a \\ (\mathbf{u}^a, g) - 1 \\ (\tilde{\mathbf{u}}^a, g) \end{pmatrix} = \mathbf{0}, \tag{5.22}$$

subject to the boundary conditions (5.9)–(5.11), (5.18)–(5.20) and

$$\tilde{\mathbf{u}}^a = 0 \quad \text{on } \Gamma_{\mathrm{D}}, \tag{5.23}$$

$$\frac{1}{Re}\frac{\partial \tilde{\mathbf{u}}^a}{\partial \mathbf{n}} - \tilde{p}^a \mathbf{n} = 0 \quad \text{on } \Gamma_{\mathrm{N}}, \tag{5.24}$$

$$\tilde{u}_x^a = 0 \quad \text{and} \quad \frac{1}{Re}\frac{\partial \tilde{u}_y^a}{\partial \mathbf{n}} - \tilde{p}^a n_y = 0 \quad \text{on } \Gamma_{\mathrm{M}}. \tag{5.25}$$

5.2. Meshes and traces. In this section we introduce the notation needed to define the interior penalty DG discretization of the primal problems (5.21), (5.9)–(5.11), (5.18)–(5.20) and (5.22), (5.9)–(5.11), (5.18)–(5.20), (5.23)–(5.25).

To this end, we assume that Ω_1 can be subdivided into a shape-regular mesh $\mathcal{T}_h = \{\kappa\}$ consisting of quadrilateral elements κ. For each $\kappa \in \mathcal{T}_h$, we denote by $\mathbf{n}_\kappa$ the unit outward normal vector to the boundary $\partial\kappa$, and by h_κ the elemental diameter. An interior edge of $\mathcal{T}_h$ is the (non-empty) one-dimensional interior of $\partial\kappa^+ \cap \partial\kappa^-$, where

κ^+ and κ^- are two adjacent elements of $\mathcal{T}_h$. Similarly, a boundary edge of $\mathcal{T}_h$ is the (non-empty) one-dimensional interior of $\partial\kappa \cap \Gamma_1$, $\Gamma_1 = \partial\Omega_1$, which consists of entire edges of $\partial\kappa$. We denote by Γ_{int} the union of all interior edges of $\mathcal{T}_h$.

Next, we define average and jump operators. To this end, let κ^+ and κ^- be two adjacent elements of $\mathcal{T}_h$, and $\mathbf{x}$ be an arbitrary point on the interior edge $e = \partial\kappa^+ \cap \partial\kappa^- \subset \Gamma_{\text{int}}$. Furthermore, let q, $\mathbf{v}$, and $\underline{\tau}$ be scalar–, vector–, and matrix–valued functions, respectively, that are smooth inside each element $\kappa^\pm$. By $(q^\pm, \mathbf{v}^\pm, \underline{\tau}^\pm)$ we denote the traces of $(q, \mathbf{v}, \underline{\tau})$ on e taken from within the interior of $\kappa^\pm$, respectively. Then, we introduce the following averages at $\mathbf{x} \in e$:

$$\{\!\{q\}\!\} = (q^+ + q^-)/2, \quad \{\!\{\mathbf{v}\}\!\} = (\mathbf{v}^+ + \mathbf{v}^-)/2, \quad \{\!\{\underline{\tau}\}\!\} = (\tau^+ + \tau^-)/2.$$

Similarly, the jumps at $\mathbf{x} \in e$ are given by

$$\begin{aligned} [\![q]\!] = q^+\mathbf{n}_{\kappa^+} + q^-\mathbf{n}_{\kappa^-}, \quad [\![\mathbf{v}]\!] = \mathbf{v}^+ \cdot \mathbf{n}_{\kappa^+} + \mathbf{v}^- \cdot \mathbf{n}_{\kappa^-}, \\ \underline{[\![\mathbf{v}]\!]} = \mathbf{v}^+ \otimes \mathbf{n}_{\kappa^+} + \mathbf{v}^- \otimes \mathbf{n}_{\kappa^-}, \quad [\![\underline{\tau}]\!] = \underline{\tau}^+\mathbf{n}_{\kappa^+} + \underline{\tau}^-\mathbf{n}_{\kappa^-}. \end{aligned}$$

On boundary edges $e \subset \Gamma_1$, we set $\{\!\{q\}\!\} = q$, $\{\!\{\mathbf{v}\}\!\} = \mathbf{v}$, $\{\!\{\underline{\tau}\}\!\} = \underline{\tau}$, $[\![q]\!] = q\mathbf{n}$, $[\![\mathbf{v}]\!] = \mathbf{v}\cdot\mathbf{n}$, $\underline{[\![\mathbf{v}]\!]} = \mathbf{v} \otimes \mathbf{n}$, and $[\![\underline{\tau}]\!] = \underline{\tau}\mathbf{n}$. Here, $\mathbf{n}$ is the unit outward normal vector to the boundary Γ_1. For matrices $\underline{\sigma}$, $\underline{\tau} \in \mathbb{R}^{m\times n}$, $m, n \geq 1$, we use the standard notation $\underline{\sigma} : \underline{\tau} = \sum_{k=1}^m \sum_{l=1}^n \sigma_{kl}\tau_{kl}$.

5.3. Discontinuous Galerkin discretization. We now introduce the DG discretization employed for the numerical approximation of both extended systems (5.21) and (5.22). To this end, for a given a mesh $\mathcal{T}_h$ and polynomial degree $p \geq 1$, we introduce the following finite element spaces

$$\begin{aligned} \mathbf{V}_{h,p} &= \{\mathbf{v} \in [L^2(\Omega_1)]^2 : \mathbf{v}|_\kappa \in [\mathcal{Q}^p(\kappa)]^2, \kappa \in \mathcal{T}_h\}, \\ Q_{h,p} &= \{q \in L^2(\Omega_1) : q|_\kappa \in \mathcal{Q}^{p-1}(\kappa), \kappa \in \mathcal{T}_h\}. \end{aligned}$$

Here, $\mathcal{Q}^p(\kappa)$ denotes the space of tensor product polynomials on κ of degree at most p in each coordinate direction. Finally, we let

$$\mathbf{V}_{S,h,p} := (\mathbf{V}_{h,p} \times Q_{h,p}) \times (\mathbf{V}_{h,p} \times Q_{h,p}) \times \mathbb{R}$$

and

$$\mathbf{V}_{H,h,p} := (\mathbf{V}_{h,p} \times Q_{h,p}) \times (\mathbf{V}_{h,p} \times Q_{h,p}) \times (\mathbf{V}_{h,p} \times Q_{h,p}) \times \mathbb{R} \times \mathbb{R}.$$

We now introduce the following symmetric version of the interior penalty method, together with a Lax–Friedrichs numerical flux approximation of the nonlinear convective terms. In the case of a steady bifurcation we have: find $\mathbf{u}_{S,h} = ((\mathbf{u}_h^0, p_h^0), (\mathbf{u}_h^a, p_h^a), Re_h^0) \in \mathbf{V}_{S,h,p}$ such that

$$\left\{ \begin{array}{lcll} A_h(\mathbf{u}_h^0, Re_h^0; \mathbf{v}_h^0) + C_h(\mathbf{u}_h^0; \mathbf{v}_h^0) + B_h(\mathbf{v}_h^0, p_h^0) & = & \ell_1(Re_h^0; \mathbf{v}_h^0), & \\ B_h(\mathbf{u}_h^0, q_h^0) & = & \ell_2(q_h^0), & \\ \hat{A}_h(\mathbf{u}_h^0, Re_h^0; \mathbf{v}_h^a) + \hat{C}_h(\mathbf{u}_h^0; \mathbf{u}_h^a, \mathbf{v}_h^a) + \hat{B}_h(\mathbf{v}_h^a, p_h^a) & = & 0, & (5.26) \\ \hat{B}_h(\mathbf{u}_h^a, q_h^a) & = & 0, & \\ \chi_h(\mathbf{u}_h^a, g) & = & 1 & \end{array} \right.$$

for all $\mathbf{v}_h = ((\mathbf{v}_h^0, q_h^0), (\mathbf{v}_h^a, q_h^a), \chi_h) \in \mathbf{V}_{S,h,p}$. While, for a Hopf bifurcation, we have: find $\mathbf{u}_{H,h} = ((\mathbf{u}_h^0, p_h^0), (\mathbf{u}_h^a, p_h^a), (\tilde{\mathbf{u}}_h^a, \tilde{p}_h^a), Re_h^0, \mu_h^a) \in \mathbf{V}_{H,h,p}$ such that

$$\begin{cases} A_h(\mathbf{u}_h^0, Re_h^0; \mathbf{v}_h^0) + C_h(\mathbf{u}_h^0; \mathbf{v}_h^0) + B_h(\mathbf{v}_h^0, p_h^0) & = & \ell_1(Re_h^0; \mathbf{v}_h^0), \\ B_h(\mathbf{u}_h^0, q_h^0) & = & \ell_2(q_h^0), \\ \hat{A}_h(\mathbf{u}_h^a, Re_h^0; \mathbf{v}_h^a) + \hat{C}_h(\mathbf{u}_h^0; \mathbf{u}_h^a, \mathbf{v}_h^a) + \hat{B}_h(\mathbf{v}_h^a, p_h^a) + \mu_h^a(\tilde{\mathbf{u}}_a^c, \mathbf{v}_h^a) & = & 0, \\ \hat{B}_h(\mathbf{u}_h^a, q_h^a) & = & 0, \\ \hat{A}_h(\tilde{\mathbf{u}}_h^s, Re_h^0; \tilde{\mathbf{v}}_h^a) + \hat{C}_h(\mathbf{u}_h^0; \tilde{\mathbf{u}}_h^a, \tilde{\mathbf{v}}_h^a) + \hat{B}_h(\tilde{\mathbf{v}}_h^a, \tilde{p}_h^a) + \mu_h^a(\mathbf{u}_h^a, \tilde{\mathbf{v}}_h^a) & = & 0, \\ \hat{B}_h(\tilde{\mathbf{u}}_h^a, \tilde{q}_h^a) & = & 0, \\ \chi_h(\mathbf{u}_h^a, g) & = & 1, \\ \varsigma_h(\tilde{\mathbf{u}}_h^a, g) & = & 0 \end{cases} \tag{5.27}$$

for all $\mathbf{v}_h = ((\mathbf{v}_h^0, q_h^0), (\mathbf{v}_h^a, q_h^a), (\tilde{\mathbf{v}}_h^a, \tilde{q}_h^a), \chi_h, \varsigma_h) \in \mathbf{V}_{H,h,p}$. In both (5.26) and (5.27) the bilinear forms A_h, $\hat{A}_h$, B_h and $\hat{B}_h$ are defined, respectively, by

$$\begin{aligned} A_h(\mathbf{u}, Re; \mathbf{v}) = \frac{1}{\mathrm{Re}} \Bigg(& \int_{\Omega_1} \nabla_h \mathbf{u} : \nabla_h \mathbf{v} \, \mathrm{d}\mathbf{x} \\ & - \int_{\Gamma_{\mathrm{int}} \cup \Gamma_{\mathrm{D}}} (\{\!\{\nabla_h \mathbf{v}\}\!\} : \underline{[\![\mathbf{u}]\!]} + \{\!\{\nabla_h \mathbf{u}\}\!\} : \underline{[\![\mathbf{v}]\!]}) \, \mathrm{d}s \\ & - \int_{\Gamma_{\mathrm{M}}} (\{\!\{\nabla \mathbf{v}_y\}\!\} \cdot [\![\mathbf{u}_y]\!] + \{\!\{\nabla \mathbf{u}_y\}\!\} \cdot [\![\mathbf{v}_y]\!]) \, \mathrm{d}s \\ & + \int_{\Gamma_{\mathrm{int}} \cup \Gamma_{\mathrm{D}}} \sigma \underline{[\![\mathbf{u}]\!]} : \underline{[\![\mathbf{v}]\!]} \, \mathrm{d}s + \int_{\Gamma_{\mathrm{M}}} \sigma [\![\mathbf{u}_y]\!] \cdot [\![\mathbf{v}_y]\!] \, \mathrm{d}s \Bigg), \\ \hat{A}_h(\mathbf{u}, Re; \mathbf{v}) = \frac{1}{\mathrm{Re}} \Bigg(& \int_{\Omega_1} \nabla_h \mathbf{u} : \nabla_h \mathbf{v} \, \mathrm{d}\mathbf{x} \\ & - \int_{\Gamma_{\mathrm{int}} \cup \Gamma_{\mathrm{D}}} (\{\!\{\nabla_h \mathbf{v}\}\!\} : \underline{[\![\mathbf{u}]\!]} + \{\!\{\nabla_h \mathbf{u}\}\!\} : \underline{[\![\mathbf{v}]\!]}) \, \mathrm{d}s \\ & - \int_{\Gamma_{\mathrm{M}}} (\{\!\{\nabla \mathbf{v}_x\}\!\} \cdot [\![\mathbf{u}_x]\!] + \{\!\{\nabla \mathbf{u}_x\}\!\} \cdot [\![\mathbf{v}_x]\!]) \, \mathrm{d}s \\ & + \int_{\Gamma_{\mathrm{int}} \cup \Gamma_{\mathrm{D}}} \sigma \underline{[\![\mathbf{u}]\!]} : \underline{[\![\mathbf{v}]\!]} \, \mathrm{d}s + \int_{\Gamma_{\mathrm{M}}} \sigma [\![\mathbf{u}_x]\!] \cdot [\![\mathbf{v}_x]\!] \, \mathrm{d}s \Bigg), \\ B_h(\mathbf{v}, q) = & - \int_{\Omega_1} q \nabla_h \cdot \mathbf{v} \, \mathrm{d}\mathbf{x} + \int_{\Gamma_{\mathrm{int}} \cup \Gamma_{\mathrm{D}}} \{\!\{q\}\!\} [\![\mathbf{v}]\!] \, \mathrm{d}s + \int_{\Gamma_{\mathrm{M}}} \{\!\{q\}\!\} \mathbf{v}_y \mathbf{n}_y \, \mathrm{d}s, \\ \hat{B}_h(\mathbf{v}, q) = & - \int_{\Omega_1} q \nabla_h \cdot \mathbf{v} \, \mathrm{d}\mathbf{x} + \int_{\Gamma_{\mathrm{int}} \cup \Gamma_{\mathrm{D}}} \{\!\{q\}\!\} [\![\mathbf{v}]\!] \, \mathrm{d}s + \int_{\Gamma_{\mathrm{M}}} \{\!\{q\}\!\} \mathbf{v}_x \mathbf{n}_x \, \mathrm{d}s, \end{aligned}$$

where the operator ∇_h is used to denote the broken gradient operator ∇, defined elementwise. The function $\sigma \in L^\infty(\Gamma_{\mathrm{int}} \cup \Gamma_1)$ is the so–called interior penalty function, which is chosen as follows: writing $\mathrm{h} \in L^\infty(\Gamma_{\mathrm{int}} \cup \Gamma_1)$ to denote the mesh function defined by

$$\mathrm{h}(\mathbf{x}) = \begin{cases} \min\{h_\kappa, h_{\kappa'}\}, & \mathbf{x} \in e = \partial\kappa \cap \partial\kappa' \subset \Gamma_{\mathrm{int}}, \\ h_\kappa, & \mathbf{x} \in e = \partial\kappa \cap \Gamma_1, \end{cases}$$

we set

$$\sigma = C_\sigma \frac{p^2}{\mathrm{h}}.$$

Here, C_σ is a positive constant which is independent of the mesh size and the polynomial degree p. To guarantee stability of the bilinear form A_h, C_σ must be chosen sufficiently large; see [5], for example, and the references cited therein.

The semilinear form C_h represents the approximation of the nonlinear convection terms and is defined by

$$C_h(\mathbf{u};\mathbf{v}) = -\int_{\Omega_1} \mathcal{F}^0(\mathbf{u}) : \nabla_h \mathbf{v}\,\mathrm{d}\mathbf{x} - \int_{\Omega_1} (\nabla\cdot\mathbf{u})\mathbf{u}\cdot\mathbf{v}\,\mathrm{d}\mathbf{x} + \int_{\Gamma_{\mathrm{int}}} \mathcal{H}(\mathbf{u}^+,\mathbf{u}^-,\mathbf{n})[\![\mathbf{v}]\!]\,\mathrm{d}s + \int_{\Gamma_1} \mathcal{H}(\mathbf{u}^+,\mathbf{u}_\Gamma,\mathbf{n})[\![\mathbf{v}]\!]\,\mathrm{d}s, \tag{5.28}$$

where $\mathcal{H}(\cdot,\cdot,\cdot)$ denotes the Lax-Friedrichs flux given by

$$\mathcal{H}(\mathbf{v},\mathbf{w},\mathbf{n}) := \frac{1}{2}\left(\mathcal{F}^0(\mathbf{v})\cdot\mathbf{n} + \mathcal{F}^0(\mathbf{w})\cdot\mathbf{n} - \alpha(\mathbf{w}-\mathbf{v})\right).$$

Here, $\alpha := \max(\mu^+,\mu^-)$, where μ^+ and μ^- are the largest eigenvalues (in absolute magnitude) of the Jacobi matrices $(\partial/\partial\mathbf{u})(\mathcal{F}^0(\cdot)\cdot\mathbf{n})$ evaluated at $\mathbf{v}$ and $\mathbf{w}$, respectively. Thereby, in this setting, we have $\alpha = 2\max(|\mathbf{v}\cdot\mathbf{n}|,|\mathbf{w}\cdot\mathbf{n}|)$.

The boundary function $\mathbf{u}_\Gamma$ is given according to the type of boundary condition imposed. To this end, we set

$$\mathbf{u}_\Gamma(\mathbf{u}) = \mathbf{g}_{\mathrm{D}} \text{ on } \Gamma_{\mathrm{D}},$$

$$\mathbf{u}_\Gamma(\mathbf{u}) = \mathbf{u}^+ \text{ on } \Gamma_{\mathrm{N}}, \quad \mathbf{u}_\Gamma(\mathbf{u}) = [u_x^+, 0]^\top \text{ on } \Gamma_{\mathrm{M}}.$$

In a similar fashion, $\hat{C}_h$ represents the approximation of the (linear) convection terms arising in the PDE problem for the nullfunction. Employing the Lax–Friedrichs flux (or simply the upwind flux function) gives

$$\hat{C}_h(\mathbf{u}^0;\mathbf{u}^a,\mathbf{v}) = -\int_{\Omega_1}\left(\mathcal{F}^a(\mathbf{u}^0,\mathbf{u}^a) : \nabla_h\mathbf{v}\right)\mathrm{d}\mathbf{x} - \frac{1}{2}\int_{\Omega_1}\left((\nabla\cdot\mathbf{u}^0)\mathbf{u}^a + (\nabla\cdot\mathbf{u}^a)\mathbf{u}^0\right)\cdot\mathbf{v}\,\mathrm{d}\mathbf{x} + \sum_{\kappa\in\mathcal{T}_h}\left(\int_{\partial\kappa\setminus\Gamma_1}\hat{\mathcal{H}}(\{\!\{\mathbf{u}^0\}\!\};\mathbf{u}^{a,+},\mathbf{u}^{a,-},\mathbf{n})\cdot\mathbf{v}^+\,\mathrm{d}s + \int_{\partial\kappa\cap\Gamma_1}\hat{\mathcal{H}}((\mathbf{u}^{0,+}+\mathbf{u}_\Gamma(\mathbf{u}^0))/2;\mathbf{u}^{a,+},\hat{\mathbf{u}}_\Gamma(\mathbf{u}^a),\mathbf{n})\cdot\mathbf{v}^+\,\mathrm{d}s\right),$$

where

$$\hat{\mathcal{H}}(\mathbf{v};\mathbf{u},\mathbf{w},\mathbf{n}) := \frac{1}{2}\left(\mathcal{F}^a(\mathbf{v};\mathbf{u})\cdot\mathbf{n} + \mathcal{F}^a(\mathbf{v};\mathbf{w})\cdot\mathbf{n} + \hat{\alpha}(\mathbf{u}-\mathbf{w})\right).$$

In this case $\hat{\alpha} = |2\mathbf{v}\cdot\mathbf{n}|$, $\mathbf{u}_\Gamma$ is as before and the new boundary function $\hat{\mathbf{u}}_\Gamma$ is given by

$$\hat{\mathbf{u}}_\Gamma(\mathbf{u}) = \mathbf{0} \text{ on } \Gamma_{\mathrm{D}},$$

$$\hat{\mathbf{u}}_\Gamma(\mathbf{u}) = \mathbf{u}^+ \text{ on } \Gamma_{\mathrm{N}}, \quad \text{and} \quad \hat{\mathbf{u}}_\Gamma(\mathbf{u}) = [0, u_y^+]^\top \text{ on } \Gamma_{\mathrm{M}}.$$

Finally, $\ell_1(\cdot;\cdot)$ and $\ell_2(\cdot)$ are given, respectively, by

$$\ell_1(Re;\mathbf{v}) = -\frac{1}{Re}\int_{\Gamma_{\mathrm{D}}} ((\mathbf{g}_{\mathrm{D}}\otimes\mathbf{n}) : \nabla\mathbf{v} - \sigma\mathbf{g}_{\mathrm{D}}\cdot\mathbf{v})\,\mathrm{d}s,$$
$$\ell_2(q) = \int_{\Gamma_{\mathrm{D}}} q\mathbf{g}_{\mathrm{D}}\cdot\mathbf{n}\,\mathrm{d}s. \tag{5.29}$$

As the chosen numerical fluxes are consistent, it then follows that the underlying DG schemes are also consistent; *i.e.*, assuming sufficient regularity of the analytical solutions $\{(\mathbf{u}^0,p^0),(\mathbf{u}^a,p^a),Re^0\}$ and $\{(\mathbf{u}^0,p^0),(\mathbf{u}^a,p^a),(\tilde{\mathbf{u}}^a,\tilde{p}^a)Re^0,\mu^a\}$ of (5.21) and (5.22), respectively, we have

$$\begin{cases} A_h(\mathbf{u}^0,Re^0;\mathbf{v}_h^0) + C_h(\mathbf{u}^0;\mathbf{v}_h^0) + B_h(\mathbf{v}_h^0,p^0) &=& \ell_1(Re_h^0;\mathbf{v}_h^0), \\ B_h(\mathbf{u}^0,q_h^0) &=& \ell_2(q_h^0), \\ \hat{A}_h(\mathbf{u}^a,Re^0;\mathbf{v}^a) + \hat{C}_h(\mathbf{u}^0;\mathbf{u}^a,\mathbf{v}^a) + \hat{B}_h(\mathbf{v}^a,p^a) &=& 0, \\ \hat{B}_h(\mathbf{u}^a,q^a) &=& 0, \\ \chi_h(\mathbf{u}^a,g) &=& 1 \end{cases} \tag{5.30}$$

for all $\mathbf{v}_h = \{(\mathbf{v}_h^0,q_h^0),(\mathbf{v}_h^a,q_h^a),\chi_h\} \in \mathbf{V}_{S,h,p}$ in the case of a steady bifurcation, while for a Hopf bifurcation, the following holds

$$\begin{cases} A(\mathbf{u}^0,Re^0;\mathbf{v}_h^0) + C_h(\mathbf{u}^0;\mathbf{v}_h^0) + B_h(\mathbf{v}_h^0,p^0) &=& \ell_1(Re_h^0;\mathbf{v}_h^0), \\ B_h(\mathbf{u}^0,q_h^0) &=& \ell_2(q_h^0,) \\ \hat{A}_h(\mathbf{u}^a,Re^0,\mathbf{v}^a) + \hat{C}_h(\mathbf{u}^0;\mathbf{u}^a,\mathbf{v}_h^a) + \hat{B}_h(\mathbf{v}_h^a,p_h^a) + \mu_h^a(\tilde{\mathbf{u}}^a,\mathbf{v}_h^a) &=& 0, \\ \hat{B}_h(\mathbf{u}^a,q_h^a) &=& 0, \\ \hat{A}_h(\tilde{\mathbf{u}}^a,Re^0;\tilde{\mathbf{v}}_h^a) + \hat{C}_h(\mathbf{u}^0;\tilde{\mathbf{u}}^a,\tilde{\mathbf{v}}_h^a) + \hat{B}_h(\tilde{\mathbf{v}}_h^a,\tilde{p}^a) + \mu_h^a(\mathbf{u}^a,\tilde{\mathbf{v}}_h^a) &=& 0, \\ \hat{B}_h(\tilde{\mathbf{u}}^a,\tilde{q}_h^a) &=& 0, \\ \chi_h(\mathbf{u}^a,g) &=& 1, \\ \varsigma_h(\tilde{\mathbf{u}}^a,g) &=& 0 \end{cases} \tag{5.31}$$

for all $\mathbf{v}_h = \{(\mathbf{v}_h^0,q_h^0),(\mathbf{v}_h^a,q_h^a),(\tilde{\mathbf{v}}_h^a,\tilde{q}_h^a),\chi_h,\varsigma_h\} \in \mathbf{V}_{H,h,p}$.

REMARK 5.1. *We point out that the mixed approximations defined in (5.26) and (5.27) are based on so-called mixed-order elements (or $(\mathcal{Q}^p)^2-\mathcal{Q}^{p-1}$ elements), where the approximation degree for the pressure is of one order lower than for the velocity. In view of the approximation properties, this pair is optimally matched. Moreover, in the context of the steady Stokes equations, it has been shown that this mixed method satisfies a discrete inf-sup condition, and is thereby well–posed; for details, see Hansbo and Larson [28], Toselli [41], Schötzau, Schwab and Toselli [38] and the references cited therein. However, by introducing suitable pressure stabilization terms, it is also possible to employ equal-order elements (or $(\mathcal{Q}^p)^2-\mathcal{Q}^p$ elements) with the same approximation degree for the velocity and the pressure; see the LDG approaches by Cockburn, Kanschat, Schötzau and Schwab [19] and Cockburn, Kanschat and Schötzau [18] for details. Finally, for the treatment of the nonlinear convection terms, we refer to the article [39] where the discretization of the time–dependent incompressible Navier–Stokes equations has been undertaken.*

6. *A posteriori* error estimation for incompressible fluid flow. We are now in a position to apply the DWR *a posteriori* error estimation technique outlined in Section 3 to the DG methods proposed above.

PROPOSITION 6.1 (Error Representation Formula). *For the steady pitchfork bifurcation, let $\mathbf{u}_S$ and $\mathbf{u}_{S,h} = ((\mathbf{u}_h^0,p_h^0),(\mathbf{u}_h^a,p_h^a),Re_h^0) \in \mathbf{V}_{S,h,p}$ denote the solutions of*

(5.21) and (5.26), respectively, and suppose that the corresponding dual problem (3.7) is well posed, with solution $\mathbf{z}_S = ((\mathbf{z}_S^0, \tau_S^0), (\mathbf{z}_S^a, \tau_S^a), z_{S,Re})$. *Then, we have*

$$Re^0 - Re_h^0 = \varepsilon_S(\mathbf{u}_S, \mathbf{u}_{S,h}; \mathbf{z}_S - \mathbf{z}_{S,h}) \equiv \sum_{\kappa \in \mathcal{T}_h} \eta_{S,\kappa} \tag{6.1}$$

for all $\mathbf{z}_{S,h} = ((\mathbf{z}_{S,h}^0, \tau_{S,h}^0), (\mathbf{z}_{S,h}^a, \tau_{S,h}^a), z_{S,Re,h}) \in \mathbf{V}_{S,h,p}$, *where*

$$\eta_{S,\kappa} = \eta_\kappa^0(Re_h^0, (\mathbf{u}_h^0, p_h^0), (\mathbf{w}_S^0, \omega_S^0)) + \eta_\kappa^a(Re_h^0, (\mathbf{u}_h^0, p_h^0), (\mathbf{u}_h^a, p_h^a), \mathbf{0}, 0, (\mathbf{w}_S^a, \omega_S^a)).$$

Similarly, let $\mathbf{u}_H$ *and* $\mathbf{u}_{H,h} = ((\mathbf{u}_h^0, p_h^0), (\mathbf{u}_h^a, p_h^a), (\tilde{\mathbf{u}}_h^a, \tilde{p}_h^a), Re_h^0, \mu_h^a) \in \mathbf{V}_{H,h,p}$ *denote the solutions of (5.22) and (5.27), respectively, with corresponding dual solution denoted by* $\mathbf{z}_H = ((\mathbf{z}_H^0, \tau_H^0), (\mathbf{z}_H^a, \tau_H^a), (\tilde{\mathbf{z}}_H^a, \tilde{\tau}_H^a), z_{H,Re}, z_{H,\mu})$, *then*

$$Re^0 - Re_h^0 = \varepsilon_H(\mathbf{u}_H, \mathbf{u}_{H,h}; \mathbf{z}_H - \mathbf{z}_{H,h}) \equiv \sum_{\kappa \in \mathcal{T}_h} \eta_{H,\kappa} \tag{6.2}$$

for all $\mathbf{z}_{H,h} = ((\mathbf{z}_{H,h}^0, \tau_{H,h}^0), (\mathbf{z}_{H,h}^a, \tau_{H,h}^a), (\tilde{\mathbf{z}}_{H,h}^a, \tilde{\tau}_{H,h}^a), z_{H,Re,h}, z_{H,\mu,h}) \in \mathbf{V}_{H,h,p}$, *where*

$$\begin{aligned}\eta_{H,\kappa} = {} & \eta_\kappa^0(Re_h^0, (\mathbf{u}_h^0, p_h^0), (\mathbf{w}_H^0, \omega_H^0)) + \eta_\kappa^a(Re_h^0, (\mathbf{u}_h^0, p_h^0), (\mathbf{u}_h^a, p_h^a), \tilde{\mathbf{u}}_h^a, \mu_h^a, \mathbf{w}_H^a, \omega_H^a) \\ & + \eta_\kappa^a(Re_h^0, (\mathbf{u}_h^0, p_h^0), (\tilde{\mathbf{u}}_h^a, \tilde{p}_h^a), \mathbf{u}_h^a, -\mu_h^a, \tilde{\mathbf{w}}_H^a, \tilde{\omega}_H^a).\end{aligned}$$

Here, for $* = S, H$, *we have*

$$\mathbf{w}_*^0 = \mathbf{z}_*^0 - \mathbf{z}_{*,h}^0, \quad \omega_*^0 = \tau_*^0 - \tau_{*,h}^0, \quad \mathbf{w}_*^a = \mathbf{z}_*^a - \mathbf{z}_{*,h}^a, \quad \omega_*^a = \tau_*^a - \tau_{*,h}^a$$

and

$$\tilde{\mathbf{w}}_H^a = \tilde{\mathbf{z}}_H^a - \tilde{\mathbf{z}}_{H,h}^a, \quad \tilde{\omega}_H^a = \tilde{\tau}_H^a - \tilde{\tau}_{H,h}^a.$$

Moreover,

$$\begin{aligned}\eta_\kappa^0(Re_h^0, (\mathbf{u}_h^0, p_h^0), (\mathbf{w}^0, \omega^0)) = {} & \int_\kappa \mathbf{R}^0(\mathbf{u}_h^0, Re_h^0; p_h^0) \cdot \mathbf{w}^0 \,\mathrm{d}x - \frac{1}{2} \int_{\partial\kappa \setminus \Gamma_1} [\![p_h^0]\!] \cdot \mathbf{w}^0 \,\mathrm{d}s \\
& + \int_{\partial\kappa \cap \Gamma_{\mathrm{N}}} \mathbf{R}_N^0(Re_h^0; \mathbf{u}_h^0, p_h^0) \cdot \mathbf{w}^{0,+} \,\mathrm{d}s \\
& + \int_{\partial\kappa \cap \Gamma_{\mathrm{M}}} \mathbf{R}_{M,x}^0(Re_h^0; \mathbf{u}_h^0, p_h^0) \mathbf{w}_x^{0,+} \,\mathrm{d}s - \frac{1}{Re_h^0} \int_{\partial\kappa \cap \Gamma_D} (\mathbf{R}_D^0(\mathbf{u}_h^0) \otimes \mathbf{n}_\kappa) : \nabla_h \mathbf{w}^{0,+} \,\mathrm{d}s \\
& + \frac{1}{Re_h^0} \int_{\partial\kappa \cap \Gamma_D} \sigma \mathbf{R}_D^0(\mathbf{u}_h^0) \cdot \mathbf{w}^{0,+} \,\mathrm{d}s + \frac{1}{Re_h^0} \int_{\partial\kappa \cap \Gamma_{\mathrm{M}}} \sigma \mathbf{R}_{M,y}^0(Re_h^0; \mathbf{u}_h^0, p_h^0) \mathbf{w}_y^{0,+} \,\mathrm{d}s \\
& - \frac{1}{Re_h^0} \int_{\partial\kappa \cap \Gamma_{\mathrm{M}}} \mathbf{R}_{M,y}^0(\mathbf{u}_h^0, p_h^0, Re_h^0) \mathbf{n}_\kappa \cdot \nabla_h \mathbf{w}_y^{0,+} \,\mathrm{d}s \\
& - \frac{1}{2Re_h^0} \int_{\partial\kappa \setminus \Gamma_1} \left\{ \underline{[\![\mathbf{u}_h^0]\!]} : \nabla \mathbf{w}_h^{0,+} - [\![\nabla \mathbf{u}_h^0]\!] \cdot \mathbf{w}^{0,+} \right\} \mathrm{d}s \\
& + \frac{1}{Re_h^0} \int_{\partial\kappa \setminus \Gamma_1} \sigma \underline{[\![\mathbf{u}_h^0]\!]} : (\mathbf{w}^{0,+} \otimes \mathbf{n}_{\kappa^+}) + \frac{1}{2} \int_{\partial\kappa \setminus \Gamma_1} \omega^{0,+} [\![\mathbf{u}_h^0]\!] \,\mathrm{d}s \\
& + \int_{\partial\kappa \cap \Gamma_{\mathrm{D}}} \omega^{0,+} \mathbf{R}_D^0(\mathbf{u}_h^0) \cdot \mathbf{n} \,\mathrm{d}s + \int_{\partial\kappa \cap \Gamma_{\mathrm{M}}} \omega^{0,+} \mathbf{R}_{M,y}^0(Re_h^0; \mathbf{u}_h^0, p_h^0) \mathbf{n}_y \,\mathrm{d}s \\
& - \int_{\partial\kappa \setminus \Gamma_1} \Big(\mathcal{F}^0(\mathbf{u}_h^0) \cdot \mathbf{n}_\kappa - \mathcal{H}(\mathbf{u}_h^{0,+}, \mathbf{u}_h^{0,-}, \mathbf{n}_\kappa) \Big) \cdot \mathbf{w}^{0,+} \,\mathrm{d}s \\
& - \int_{\partial\kappa \cap \Gamma_1} \Big(\mathcal{F}^0(\mathbf{u}_h^0) \cdot \mathbf{n}_\kappa - \mathcal{H}(\mathbf{u}_h^{0,+}, \mathbf{u}_\Gamma(\mathbf{u}_h^{0,+}), \mathbf{n}_\kappa) \Big) \cdot \mathbf{w}^{0,+} \,\mathrm{d}s,\end{aligned} \tag{6.3}$$

where, $\mathbf{R}^0(\mathbf{u}_h^0, Re_h^0; p_h^0)|_\kappa = \left[\mathcal{L}^0(\mathbf{u}_h^0, Re_h^0; p_h^0), \nabla\cdot\mathbf{u}_h^0\right]^\top|_\kappa$ *denotes the elementwise residual and* $\mathbf{R}_{\mathrm{D}}^0(\mathbf{u}_h^0)$, $\mathbf{R}_{\mathrm{N}}^0(Re_h^0; \mathbf{u}_h^0, p_h^0)$ *and* $\mathbf{R}_{\mathrm{M}}^0(Re_h^0; \mathbf{u}_h^0, p_h^0)$ *are the Dirichlet, Neumann and mixed* boundary residuals*, respectively, given by*

$$\mathbf{R}_{\mathrm{D}}^0(\mathbf{u}_h^0)|_{\partial\kappa\cap\Gamma_{\mathrm{D}}} = (\mathbf{u}_h^+ - \mathbf{g}_{\mathrm{D}})|_{\partial\kappa\cap\Gamma_{\mathrm{D}}},$$

$$\mathbf{R}_{\mathrm{N}}^0(Re_h^0; \mathbf{u}_h^0, p_h^0)|_{\partial\kappa\cap\Gamma_{\mathrm{N}}} = \frac{1}{Re_h^0}\frac{\partial \mathbf{u}_h^{0,+}}{\partial \mathbf{n}} - p_h^{0,+}\mathbf{n}|_{\partial\kappa\cap\Gamma_{\mathrm{N}}},$$

$$\mathbf{R}_{\mathrm{M}}^0(Re_h^0; \mathbf{u}_h^0, p_h^0)|_{\partial\kappa\cap\Gamma_{\mathrm{M}}} = \left[\frac{1}{Re_h^0}\frac{\partial \mathbf{u}_{h,x}^{0,+}}{\partial \mathbf{n}} - p_h^{0,+}\mathbf{n}_x, \mathbf{u}_{h,y}^{0,+}\right]^\top\Bigg|_{\partial\kappa\cap\Gamma_{\mathrm{M}}}.$$

Similarly, η_κ^a *is given by*

$$\begin{aligned}
&\eta_\kappa^a(Re_h^0, (\mathbf{u}_h^0, p_h^0), (\mathbf{u}_h^a, p_h^a), \boldsymbol{\phi}_h, \mu_h, (\mathbf{w}^a, \omega^a)) = \int_\kappa \mathbf{R}^a(\mathbf{u}_h^0, Re_h^0; \mathbf{u}_h^a, p_h^a, \mu_h, \boldsymbol{\phi}_h)\cdot\mathbf{w}^a\,\mathrm{d}x\\
&-\frac{1}{2}\int_{\partial\kappa\setminus\Gamma_1}[\![p_h^a]\!]\cdot\mathbf{w}^a\,\mathrm{d}s + \int_{\partial\kappa\cap\Gamma_{\mathrm{N}}}\mathbf{R}_N^a(Re_h^0; \mathbf{u}_h^a, p_h^a)\cdot\mathbf{w}^{a,+}\,\mathrm{d}s\\
&+\int_{\partial\kappa\cap\Gamma_{\mathrm{M}}}\mathbf{R}_{M,y}^a(Re_h^0; \mathbf{u}_h^a, p_h^a)\mathbf{w}_y^{a,+}\,\mathrm{d}s - \frac{1}{Re_h^0}\int_{\partial\kappa\cap\Gamma_D}(\mathbf{R}_D^a(\mathbf{u}_h^a)\otimes\mathbf{n}_\kappa):\nabla_h\mathbf{w}^{a,+}\,\mathrm{d}s\\
&+\frac{1}{Re_h^0}\int_{\partial\kappa\cap\Gamma_D}\sigma\mathbf{R}_D^a(\mathbf{u}_h^a)\cdot\mathbf{w}^{a,+}\,\mathrm{d}s + \frac{1}{Re}\int_{\partial\kappa\cap\Gamma_{\mathrm{M}}}\sigma\mathbf{R}_{M,x}^a(Re_h^0; \mathbf{u}_h^a, p_h^a)\mathbf{w}_x^{0,+}\,\mathrm{d}s\\
&-\frac{1}{Re_h^0}\int_{\partial\kappa\cap\Gamma_{\mathrm{M}}}\mathbf{R}_{M,x}^0(Re_h^0; \mathbf{u}_h^a, p_h^a)\mathbf{n}_\kappa\cdot\nabla_h\mathbf{w}_x^{a,+}\,\mathrm{d}s\\
&-\frac{1}{2Re_h^0}\int_{\partial\kappa\setminus\Gamma_1}\left\{\underline{[\![\mathbf{u}_h^a]\!]}:\nabla\mathbf{w}^{a,+} - [\![\nabla\mathbf{u}_h^a]\!]\cdot\mathbf{w}^{a,+}\right\}\mathrm{d}s\\
&+\frac{1}{Re}\int_{\partial\kappa\setminus\Gamma_1}\sigma\underline{[\![\mathbf{u}_h^a]\!]}:(\mathbf{w}^{a,+}\otimes\mathbf{n}_\kappa)\,\mathrm{d}s + \frac{1}{2}\int_{\partial\kappa\setminus\Gamma_1}\omega^{a,+}[\![\mathbf{u}_h^a]\!]\,\mathrm{d}s\\
&+\int_{\partial\kappa\cap\Gamma_{\mathrm{D}}}\omega^{a,+}\mathbf{R}_D^a(\mathbf{u}_h^a)\cdot\mathbf{n}\,\mathrm{d}s + \int_{\partial\kappa\cap\Gamma_{\mathrm{M}}}\omega^{a,+}\mathbf{R}_{M,x}^a(Re_h^0; \mathbf{u}_h^a, p_h^a)\mathbf{n}_x\,\mathrm{d}s\\
&-\int_{\partial\kappa\setminus\Gamma_1}\Big(\mathcal{F}^a(\mathbf{u}_h^0; \mathbf{u}_h^a)\cdot\mathbf{n}_\kappa - \hat{\mathcal{H}}(\{\!\{\mathbf{u}_h^0\}\!\}; \mathbf{u}^{a,+}, \mathbf{u}^{a,-}, \mathbf{n})\Big)\cdot\mathbf{w}^{a,+}\,\mathrm{d}s\\
&-\int_{\partial\kappa\cap\Gamma_1}\Big(\mathcal{F}^a(\mathbf{u}_h^0; \mathbf{u}_h^a)\cdot\mathbf{n}_\kappa - \hat{\mathcal{H}}((\mathbf{u}^{0,+} + \mathbf{u}_\Gamma(\mathbf{u}^0))/2; \mathbf{u}^{a,+}, \hat{\mathbf{u}}_\Gamma(\mathbf{u}^a), \mathbf{n})\Big)\cdot\mathbf{w}^{a,+}\,\mathrm{d}s.
\end{aligned}$$

Here, we write

$$\mathbf{R}^a(\mathbf{u}_h^0, Re_h^0; \mathbf{u}_h^a, p_h^a, \mu_h, \boldsymbol{\phi}_h)|_\kappa = \left[\mathcal{L}^a(\mathbf{u}_h^0, Re_h^0; \mathbf{u}_h^a, p_h^a) + \mu_h\boldsymbol{\phi}_h, \nabla\cdot\mathbf{u}_h^a\right]^\top|_\kappa$$

to denote the elementwise residual and $\mathbf{R}_{\mathrm{D}}^a(\mathbf{u}_h^a)$, $\mathbf{R}_{\mathrm{N}}^a(Re_h^0; \mathbf{u}_h^a, p_h^a)$ *and* $\mathbf{R}_{\mathrm{M}}^a(Re_h^0; \mathbf{u}_h^a, p_h^a)$ *are the Dirichlet, Neumann and mixed* boundary residuals *of the nullfunctions, respectively, given by*

$$\mathbf{R}_{\mathrm{D}}^a(\mathbf{u}_h^a)|_{\partial\kappa\cap\Gamma_{\mathrm{D}}} = \mathbf{u}_h^+|_{\partial\kappa\cap\Gamma_{\mathrm{D}}},$$

$$\mathbf{R}_{\mathrm{N}}^a(Re_h^0; \mathbf{u}_h^a, p_h^a)|_{\partial\kappa\cap\Gamma_{\mathrm{N}}} = \frac{1}{Re_h^0}\frac{\partial \mathbf{u}_h^{m,+}}{\partial \mathbf{n}} - p_h^{m,+}\mathbf{n}|_{\partial\kappa\cap\Gamma_{\mathrm{N}}},$$

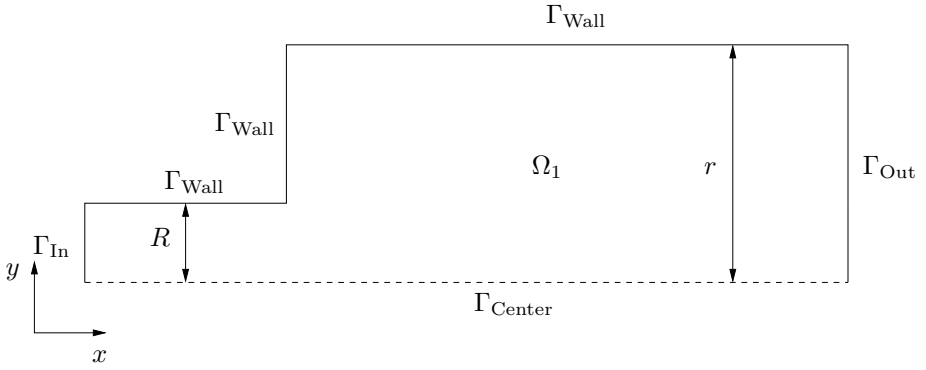

FIG. 7.1. *Example 1: Half Channel with a Sudden Expansion*

$$\mathbf{R}^a_{\mathrm{M}}(Re^0_h;\mathbf{u}^a_h,p^a_h)|_{\partial\kappa\cap\Gamma_{\mathrm{M}}}=\left[\mathbf{u}^{m,+}_{h,x},\frac{1}{Re^0_h}\frac{\partial\mathbf{u}^{m,+}_{h,y}}{\partial\mathbf{n}}-p^{m,+}_h\mathbf{n}_y\right]^{\top}\Bigg|_{\partial\kappa\cap\Gamma_{\mathrm{M}}}.$$

7. Numerical experiments. In this section we present a series of numerical examples to demonstrate the practical performance of the proposed *a posteriori* error estimator derived in Proposition 6.1 within an automatic adaptive refinement procedure which is based on employing 1-irregular quadrilateral elements. Here, the elements are marked for refinement/derefinement on the basis of the size of the elemental error indicators, $|\eta_{S,\kappa}|$ in the case of a steady bifurcation and $|\eta_{H,\kappa}|$ for a Hopf bifurcation, using the fixed fraction refinement algorithm with refinement and derefinement fractions set to 25% and 10%, respectively. In each of the examples shown in this section, we set $C_\sigma = 10$, $p = 2$, and $\hat{p} = 3$.

Throughout this section, the underlying linear systems are solved using the MUltifrontal Massively Parallel Solver, see [2, 3, 4] for details. In order to obtain the initial guesses for the damped Newton method, once a base solution has been obtained for a specific Reynolds number, we employ the Arnoldi Package (ARPACK) of Lehoucq, Sorensen and Yang [35] to calculate the most dangerous eigenvalue and corresponding eigenfunctions. ARPACK is most adept at finding highly separated eigenvalues with large magnitude and not necessarily those with small real part that determine linear stability. To overcome this difficulty we employ the modified Cayley transform outlined in Cliffe *et al.* [12], for example.

7.1. Example 1. In this first example we consider the flow of an incompressible fluid in a channel with a sudden expansion; the ratio of the half-width of expanded section of the channel, r, to that of the inlet section channel, R, being set to 3:1 and the outlet being sufficiently long to allow Poiseuille flow to have fully developed at the exit, see Figure 7.1. On entry, Γ_{In}, the flow is also assumed to be Poiseuille; no slip Dirichlet conditions are imposed on Γ_{Wall}, a Neumann condition is enforced on Γ_{Out} and the mixed boundary condition is imposed on Γ_{Center}.

In this setting it is well known, see [23], that at around $Re = 40$ there is a steady symmetry breaking bifurcation, where a real eigenvalue crosses the imaginary axis. In fact, computations on very fine grids reveal that the critical Reynolds number has the value $Re^0 \approx 40.55787701084642$. We begin with a uniform starting grid, comprising 640 elements and perform 8 adaptive refinement steps based on employing

No. Elements	Base DOF	Null DOF	Re_h^0	$\lvert Re^0 - Re_h^0\rvert$	τ
640	14080	14080	40.4923	6.557E-02	1.83
1129	24838	24838	40.5410	1.689E-02	2.34
2029	44638	44638	40.5480	9.832E-03	1.99
3601	79222	79222	40.5516	6.225E-03	1.63
6130	134860	134860	40.5542	3.696E-03	1.40
10501	231022	231022	40.5558	2.055E-03	1.27
17980	395560	395560	40.5568	1.103E-03	1.17
30796	677512	677512	40.5573	5.785E-04	1.09
52654	1158388	1158388	40.5576	3.064E-04	1.00

TABLE 7.1
Example 1: Adaptive algorithm

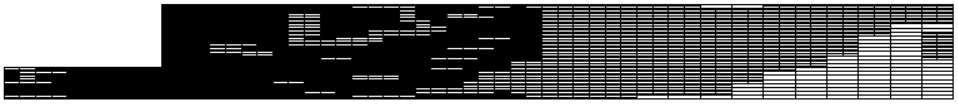

FIG. 7.2. *Example 1: Full mesh after 5 refinement steps*

the fixed fraction refinement strategy. Table 7.1 shows the number of elements, the number of degrees of freedom in computing the primal base solution and the primal null function, the error in the critical Reynolds number and the error effectivities $\tau = |\sum_{\kappa\in\mathcal{T}_h}\eta_{S,\kappa}|/|Re^0 - Re_h^0|$. We notice immediately that, as the mesh is refined, the error effectivities tend to unity, indicating that our error indicator is performing extremely well.

Figures 7.2 and 7.3(a) show the mesh after 5 refinement steps; the latter shows the detail of the mesh in the vicinity of the reentrant corner. Although refinement has been performed throughout the computational domain, we observe from Figure 7.3(a) that the majority of the refinement has been performed in the vicinity of the reentrant corner, as we would expect. For brevity we do not show plots of all the components of the primal base and dual solution and primal and dual eigenfunctions; instead, we show a contour plot of the y–component of the dual base solution in Figure 7.3(b), in order to indicate how the refinement has been directed towards the structure of the dual solution.

Finally, in Figure 7.4 we show a comparison of the adaptive refinement strategy with a uniform mesh refinement algorithm; here the error in the computed critical Reynolds number is plotted against the number of degrees of freedom (in the primal base problem) for both strategies. We notice immediately that the adaptive refinement strategy is superior to uniform refinement, in the sense that, for a given number of degrees of freedom, the error in the critical Reynolds number computed on the adaptively refined meshes is always less than the corresponding quantity computed using simply uniform refinement of the mesh. Indeed, on the final grid we notice over an order of magnitude reduction in the error when the former strategy is employed in comparison to the case when uniform mesh refinement is exploited.

7.2. Example 2. In this second example we consider flow in a channel with a cylinder centered on the midline of the channel partially blocking the flow; the radius of the cylinder is r and the half-width of the channel is R, see Figure 7.5. We consider a blockage ratio $r:R = 1:2$, with Poiseuille flow on entry, no slip conditions on Γ_{Wall}

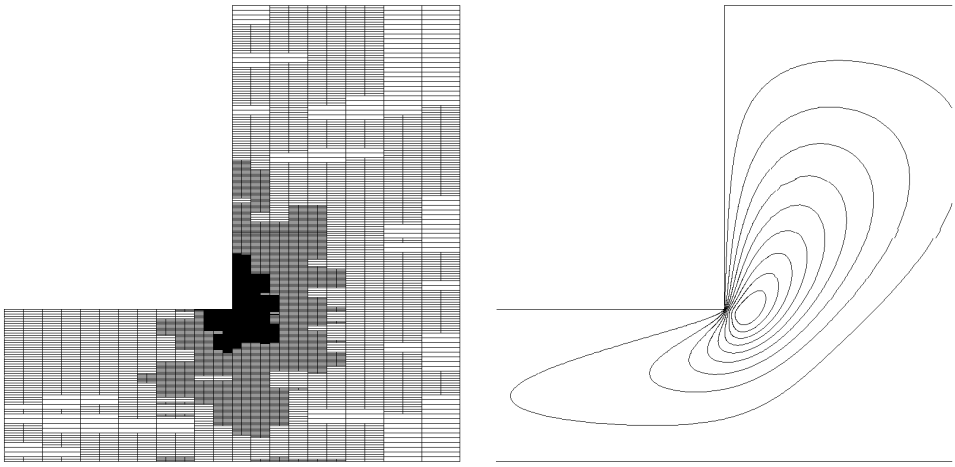

FIG. 7.3. *Example 1: Detail near expansion (a) Mesh after 5 refinement steps (b) Contour plot of* $\mathbf{z}_y^0$

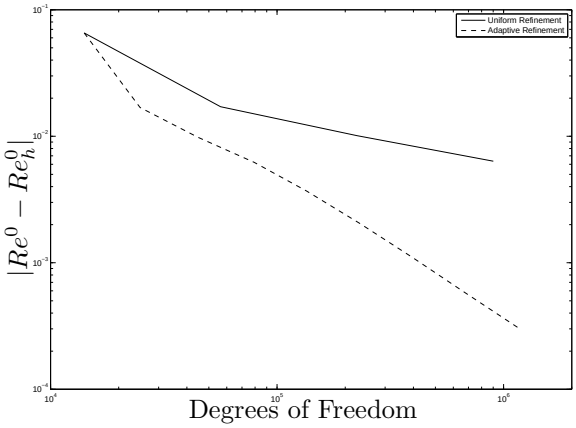

FIG. 7.4. *Example 1: Convergence of the error in the approximation of the critical Re.*

and Γ_{B}, a Neumann condition on Γ_{Out} and a mixed condition on Γ_{Center}. For this configuration a symmetry breaking Hopf bifurcation occurs at around $Re = 120$, see [17]. In fact, computations on a fine grid reveal that $Re^0 \approx 123.6378680537182$.

An initial starting grid with 924 elements, which is fitted around the blockage, is employed. The performance of the proposed adaptive algorithm is presented in Table 7.2. As before, we show in tabular form the number of elements, the number of degrees of freedom for both the primal base and primal null solutions, the error in the critical Reynolds number and the error effectivities $\tau = |\sum_{\kappa \in \mathcal{T}_h} \eta_{H,\kappa}|/|Re^0 - Re_h^0|$. In this case we see an improvement of the effectivities in comparison to the previous example; in this case the effectivities tend to unity in much fewer refinement steps, this possibly being due to greater regularity of the dual base and null solutions.

Figures 7.6(a) and 7.7(a) show the adaptively refined mesh after 5 refinement

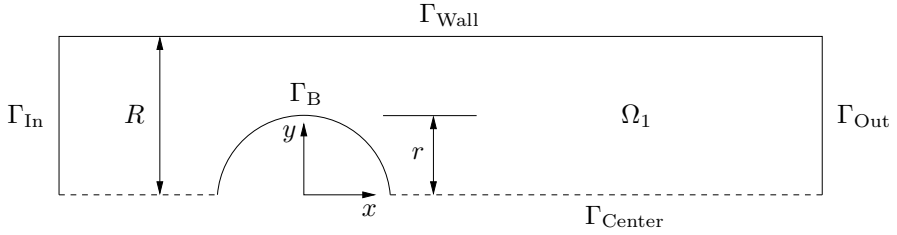

FIG. 7.5. *Example 2: Half Channel with a Cylindrical Blockage*

No. Elements	Base DOF	Null DOF	Re_h^0	$\lvert Re^0 - Re_h^0 \rvert$	τ
924	20328	20328	139.951	16.314	1.02
1632	35904	35904	124.234	5.963E-01	1.12
2898	63756	63756	123.659	2.110E-02	0.98
5235	115170	115170	123.636	1.708E-03	1.10
9420	207240	207240	123.638	2.450E-04	1.18
16647	366234	366234	123.638	1.972E-04	1.00

TABLE 7.2
Example 2: Adaptive algorithm.

steps, the former showing the full extent of the mesh, while the latter shows the mesh detail near to the blockage. We notice that the majority of refinement has been performed downstream of the blockage, with substantially less being undertaken upstream. Figures 7.6(b) and 7.7(b) show contour plots of the x–component of the dual null solution $\mathbf{z}^a$ over the same portion of the domain as depicted in Figures 7.6(a) and 7.7(a), respectively. It can be seen that some of the mesh refinement in the right portion of the domain has been carried out in response to the fine structures present in the dual null solution.

Finally, we again compare the error in the computed critical Reynolds number, using both the proposed adaptive refinement strategy and an algorithm exploiting uniform mesh refinement; see Figure 7.8. As in the previous example, we observe that the adaptive refinement strategy is superior to uniform refinement, in the sense that, for a given number of degrees of freedom, the error in the critical Reynolds number computed on the adaptively refined meshes is always less than the corresponding quantity computed using simply uniform refinement of the mesh. Indeed, on the final grid we notice over two orders of magnitude reduction in the error when the former strategy is employed in comparison to the case when uniform mesh refinement is exploited.

8. Conclusions. In this article we have considered the reliable computation of a given critical parameter at which a nonlinear problem undergoes a steady or Hopf bifurcation. Particular attention has been devoted to the *a posteriori* error estimation and adaptive mesh refinement of DG finite element approximations of the bifurcation problem associated with the steady incompressible Navier–Stokes equations. On the basis of exploiting a duality argument, reliable error estimates of the critical Reynolds number at which a steady pitchfork or Hopf bifurcation occurs when the underlying physical system possesses reflectional or Z_2 symmetry have been developed. The application of these bounds within an automatic adaptive refinement strategy clearly highlights the flexibility of the proposed *a posteriori* error indicator for accurately

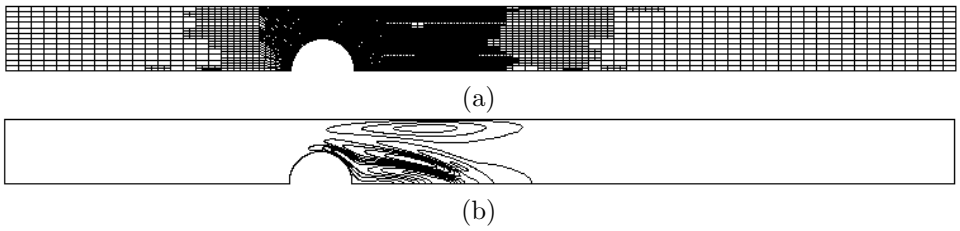

FIG. 7.6. *Example 2: (a) Full mesh after* 5 *refinement steps and (b) Contour plot of* $\mathbf{z}_x^a$

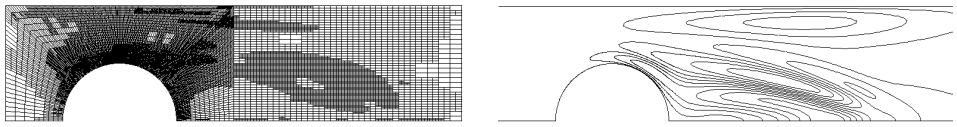

FIG. 7.7. *Example 2: Detail near blockage (a) Mesh after* 5 *refinement steps (b) Contour plot of* $\mathbf{z}_x^a$

locating both steady pitchfork and Hopf bifurcations. The extension of the ideas developed in this article to bifurcation problems involving incompressible fluid flow in systems with $O(2)$-symmetry will be developed in the companion article [13].

Acknowledgments. KAC, PH, and EJCH gratefully acknowledge the financial support of the EPSRC under the grant EP/E013724. In addition, all of the authors acknowledge the support of the EPSRC under the grant EP/F01340X.

REFERENCES

[1] M. Ainsworth and J.T. Oden. *A Posteriori Error Estimation in Finite Element Analysis.* Series in Computational and Applied Mathematics. Elsevier, 1996.

[2] P. R. Amestoy, I. S. Duff, J. Koster, and J.-Y. L'Excellent. A fully asynchronous multifrontal solver using distributed dynamic scheduling. *SIAM Journal on Matrix Analysis and Applications*, 23(1):15–41, 2001.

[3] P. R. Amestoy, I. S. Duff, and J.-Y. L'Excellent. Multifrontal parallel distributed symmetricand unsymmetric solvers. *Comput. Methods Appl. Mech. Eng.*, 184:501–520, 2000.

[4] P. R. Amestoy, A. Guermouche, J.-Y. L'Excellent, and S. Pralet. Hybrid scheduling for the parallel solution of linear systems. *Parallel Computing*, 32(2):136–156, 2006.

[5] D.N. Arnold, F. Brezzi, B. Cockburn, and L.D. Marini. Unified analysis of discontinuous Galerkin methods for elliptic problems. *SIAM J. Numer. Anal.*, 39:1749–1779, 2001.

[6] P.J. Aston. Analysis and computation of symmetry-breaking bifurcation and scaling laws using group theoretic methods. *SIAM J. Math. Anal.*, 22:139–152, 1991.

[7] I. Babuška and J. Osborn. A posteriori error estimates for the finite element method. *Internat. J. Numer. Methods Engrg.*, 12:1597–1615, 1978.

[8] I. Babuška and Tsuchiya. A posteriori error estimates of the finite element solutions of parameterized nonlinear equations. Technical report, University of Maryland, 1992.

[9] W. Bangerth and R. Rannacher. *Adaptive Finite Element Methods for Differential Equations (Lectures in Mathematics, ETH Zurich).* Birkhauser Verlag AG, 2003.

[10] R. Becker and R. Rannacher. An optimal control approach to a-posteriori error estimation in finite element methods. In A. Iserles, editor, *Acta Numerica*, pages 1–102. Cambridge University Press, 2001.

[11] F. Brezzi, J. Rappaz, and P.A. Raviart. Finite dimensional approximation of non-linear problems .3. Simple bifurcation points. *Numer. Math.*, 38(1):1–30, 1981.

[12] K.A. Cliffe, T.J. Garratt, and A. Spence. Eigenvalues of the discretized Navier-Stokes equations with application to the detection of Hopf bifurcations. *Adv. Comp. Math.*, 1:337–356, 1993.

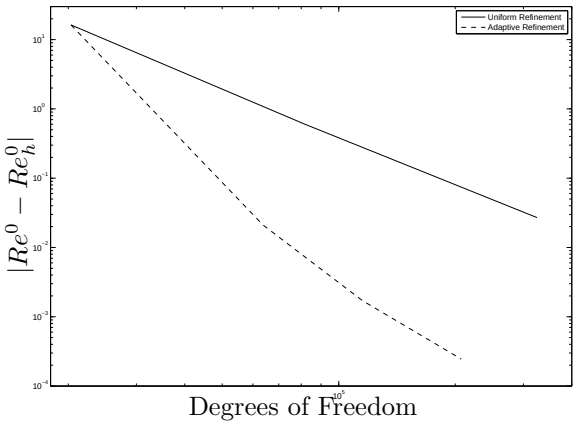

FIG. 7.8. *Example 2: Convergence of the error in the approximation of the critical Re.*

[13] K.A. Cliffe, E. Hall, and P. Houston. Adaptivity and a posteriori error control for bifurcation problems III: Incompressible fluid flow in open systems with O(2) symmetry. In preparation.

[14] K.A. Cliffe, E. Hall, and P. Houston. Adaptive discontinuous Galerkin methods for eigenvalue problems arising in incompressible fluid flows. *SIAM J. Sci. Comput.*, 31:4607–4632, 2010.

[15] K.A. Cliffe, E. Hall, P. Houston, E.T. Phipps, and A.G. Salinger. Adaptivity and a posteriori error control for bifurcation problems I: The Bratu problem. *Commun. Comput. Phys.* In press.

[16] K.A. Cliffe, A. Spence, and S.J. Tavener. O(2)-symmetry breaking bifurcation: with application to the flow past a sphere in a pipe. *Internat. J. Numer. Methods Fluids*, 32:175–200, 2000.

[17] K.A. Cliffe and S.J. Tavener. The effect of cylinder rotation and blockage ratio on the onset of periodic flows. *J. Fluid Mech.*, 501:125–133, 2004.

[18] B. Cockburn, G. Kanschat, and D. Schötzau. The local discontinuous Galerkin method for the Oseen equations. *Math. Comp.*, 73:569–593, 2004.

[19] B. Cockburn, G. Kanschat, D. Schötzau, and C. Schwab. Local discontinuous Galerkin methods for the Stokes system. *SIAM J. Numer. Anal.*, 40:319–343, 2002.

[20] R.G. Durán, L. Gastaldi, and C. Padra. A posteriori error estimators for mixed approximations of eigenvalue problems. *Math. Models Methods Appl. Sci.*, 9:1165–1178, 1999.

[21] R.G. Durán, C. Padra, and R. Rodriguez. A posteriori error estimates for the finite element approximation of eigenvalue problems. *Math. Models Methods Appl. Sci.*, 13(8):1219–1229, 2003.

[22] K. Eriksson, D. Estep, P. Hansbo, and C. Johnson. Introduction to adaptive methods for differential equations. In A. Iserles, editor, *Acta Numerica*, pages 105–158. Cambridge University Press, 1995.

[23] R.M. Fearn, T. Mullin, and K.A. Cliffe. Nonlinear flow phenomena in a symmetric sudden expansion. *J. Fluid Mech.*, 211:595–608, 1990.

[24] S. Giani and I. Graham. A convergent adaptive method for elliptic eigenvalue problems. *SIAM J. Numer. Anal.*, 47:1067–1091, 2009.

[25] M. Golubitsky and D.G. Schaeffer. *Singularities and Groups in Bifurcation Theory, Vol I.* Springer, New York, 1985.

[26] M. Golubitsky, I. Stewart, and D.G. Schaeffer. *Singularities and Groups in Bifurcation Theory, Vol II.* Springer, New York, 1988.

[27] A. Griewank and G. Reddien. The calculation of Hopf points by a direct method. *IMA J. Numer. Anal.*, 3(3):295–303, 1983.

[28] P. Hansbo and M.G. Larson. Discontinuous finite element methods for incompressible and nearly incompressible elasticity by use of Nitsche's method. *Comput. Methods Appl. Mech. Engrg.*, 191:1895–1908, 2002.

[29] V. Heuveline and R. Rannacher. A posteriori error control for finite element approximations of elliptic eigenvalue problems. *Adv. Comp. Math.*, 15:107–138, 2001.

[30] P. Houston and E. Süli. Adaptive finite element approximation of hyperbolic problems. In

T. Barth and H. Deconinck, editors, *Error Estimation and Adaptive Discretization Methods in Computational Fluid Dynamics. Lect. Notes Comput. Sci. Engrg.*, volume 25, pages 269–344. Springer, 2002.

[31] A.D. Jepson. *Numerical Hopf Bifurcation*. PhD thesis, Caltech, Pasadena, 1981.

[32] H.B. Keller. *Numerical Solution of Bifurcation and Nonlinear Eigenvalue Problems*. Academic Press, New York, 1977.

[33] M.G. Larson. A posteriori and a priori error analysis for finite element approximations of self–adjoint elliptic eigenvalue problems. *SIAM J. Numer. Anal.*, 38:608–625, 2000.

[34] M.G. Larson and T.J. Barth. A posteriori error estimation for discontinuous Galerkin approximations of hyperbolic systems. In B. Cockburn, G.E. Karniadakis, and C.-W. Shu, editors, *Discontinuous Galerkin Methods: Theory, Computation and Applications, Lecture Notes in Computational Science and Engineering, Vol. 11*. Springer, 2000.

[35] R.B. Lehoucq, D.C. Sorensen, and C. Yang. *ARPACK USERS GUIDE: Solution of Large Scale Eigenvalue Problems by Implicitly Restarted Arnoldi Methods*. SIAM, Philadelphia, PA, 1998.

[36] C. Lovadina, M. Lyly, and R. Stenberg. A posteriori estimates for the Stokes eigenvalue problem. *Num. Meth. Part. Diff. Eqs.*, 24:244–257, 2009.

[37] C. Nystedt. A priori and a posteriori error estimates and adaptive finite element methods for a model eigenvalue problem. Technical Report 1995-05, Chalmers Finite Element Center, Chalmers University, 1995.

[38] D. Schötzau, C. Schwab, and A. Toselli. Mixed *hp*-DGFEM for incompressible flows. *SIAM J. Numer. Anal.*, 40:2171–2194, 2003.

[39] K. Shahbazi, P.F. Fischer, and C.R. Ethier. A high-order discontinuous Galerkin method for the unsteady incompressible Navier–Stokes equations. *J. Comput. Phys.*, 222(1):391–407, 2007.

[40] B. Szabó and I. Babuška. *Finite Element Analysis*. J. Wiley & Sons, New York, 1991.

[41] A. Toselli. *hp*-Discontinuous Galerkin approximations for the Stokes problem. *Math. Models Methods Appl. Sci.*, 12:1565–1616, 2002.

[42] A. Vanderbauwhede. *Local Bifurcation and Symmetry*. Pitman, 1982.

[43] R. Verfürth. A posteriori error estimates for nonlinear problems. *Math. Comp.*, 62:445–475, 1989.

[44] R. Verfürth. *A Review of a Posteriori Error Estimation and Adaptive Mesh-Refinement Techniques*. B.G. Teubner, Stuttgart, 1996.

[45] T.F. Walsh, G.M. Reese, and U.L. Hetmaniuk. Explicit a posteriori error estimates for eigenvalue analysis of heterogeneous elastic structures. *Comput. Methods Appl. Mech. Engrg.*, 196:3614–3623, 2007.

[46] B. Werner and V. Janovsky. Computation of Hopf branches bifurcating from Takens-Bogdanov points for problems with symmetries. In R. Seydel, F.W. Schneider, T. Kupper, and H. Troger, editors, *Bifurcaton and Chaos: Analysis, Algorithms, Applications*, volume 97 of *International series of numerical mathematics*, pages 377–388, 1991.

[47] B. Werner and A. Spence. The computation of symmetry-breaking bifurcation points. *SIAM J. Numer. Anal.*, 21:388–399, 1984.